New Insights Into the Roles of NADPH Oxidases in Sexual Development and Ascospore Germination in *Sordaria macrospora*

Daniela Elisabeth Dirschnabel,* Minou Nowrousian,* Nallely Cano-Domínguez,† Jesus Aguirre,† Ines Teichert,* and Ulrich Kück*,[1]

*Lehrstuhl für Allgemeine und Molekulare Botanik, Ruhr Universität Bochum, 44780 Bochum, Germany, and †Departamento de Biología Celular y Desarrollo, Instituto de Fisiología Celular, Universidad Nacional Autónoma de México, Apartado Postal 70-242, 04510 México D. F., México

ABSTRACT NADPH oxidase (NOX)-derived reactive oxygen species (ROS) act as signaling determinants that induce different cellular processes. To characterize NOX function during fungal development, we utilized the genetically tractable ascomycete *Sordaria macrospora*. Genome sequencing of a sterile mutant led us to identify the NADPH oxidase encoding *nox1* as a gene required for fruiting body formation, regular hyphal growth, and hyphal fusion. These phenotypes are shared by Δnor1, lacking the NOX regulator NOR1. Further phenotypic analyses revealed a high correlation between increased ROS production and hyphal fusion deficiencies in Δnox1 and other sterile mutants. A genome-wide transcriptional profiling analysis of mycelia and isolated protoperithecia from wild type and Δnox1 revealed that *nox1* inactivation affects the expression of genes related to cytoskeleton remodeling, hyphal fusion, metabolism, and mitochondrial respiration. Genetic analysis of Δnox2, lacking the NADPH oxidase 2 gene, Δnor1, and transcription factor deletion mutant Δste12, revealed a strict melanin-dependent ascospore germination defect, indicating a common genetic pathway for these three genes. We report that *gsa3*, encoding a G-protein α-subunit, and *sac1*, encoding cAMP-generating adenylate cyclase, act in a separate pathway during the germination process. The finding that cAMP inhibits ascospore germination in a melanin-dependent manner supports a model in which cAMP inhibits NOX2 activity, thus suggesting a link between both pathways. Our results expand the current knowledge on the role of NOX enzymes in fungal development and provide a frame to define upstream and downstream components of the NOX signaling pathways in fungi.

DURING sexual reproduction, filamentous fungi generate complex fruiting bodies that contain and protect meiosporangia. We used the ascomycetous model fungus *Sordaria macrospora* to identify genes directly involved in fruiting body development (Kück *et al.* 2009; Engh *et al.* 2010; Kück *et al.* 2009). Due to its homothallic life style, *S. macrospora* is able to complete the sexual life cycle without the mating of strains with opposite sex, and therefore, fruiting body-deficient mutants can be recognized directly without the need for crossing experiments. In earlier work, we generated sterile mutants showing a developmental block after formation of young fruiting bodies (protoperithecia), but being unable to generate mature perithecia, and referred to these mutants as pro. Recently, we have applied next-generation genome re-sequencing to identify the genes affected in some of these mutants (Nowrousian *et al.* 2012). Based on this approach, we now have characterized mutant pro32 and show that it carries a mutation in the *nox1* gene encoding NAPDH oxidase 1 (NOX1).

NADPH oxidase (NOX) enzymes are transmembrane proteins that are highly conserved among eukaryotes and produce reactive oxygen species (ROS) through the oxidation of NADPH (Lambeth 2004; Kawahara and Lambeth 2007). ROS have long been recognized as damaging agents due to uncontrolled oxidizing reactions with DNA, RNA, proteins, and lipids (Halliwell and Gutteridge 2007). However, there is increasing evidence

doi: 10.1534/genetics.113.159368
Manuscript received November 5, 2013; accepted for publication January 3, 2014; published Early Online January 9, 2014.
Supporting information is available online at http://www.genetics.org/lookup/suppl/doi:10.1534/genetics.113.159368/-/DC1.
The RNA-seq reads and derived expression ratios were submitted to the GEO database (accession no. GSE49363). Raw sequence data from sequencing mutant pro32 (pro32/fus) and wild type (wt_3) were submitted to the NCBI sequence read archive (accession no. SRP033637).
This article is dedicated to Karl Esser (Bochum) on the occasion of his 90th birthday.
[1]Corresponding author: Lehrstuhl für Allgemeine und Molekulare Botanik, Ruhr-Universität Bochum, ND7/131, Universitätsstraße 150, 44780 Bochum, Germany. E-mail: ulrich.kueck@rub.de

that ROS act as signaling determinants that induce different cellular processes (Scott and Eaton 2008; Aguirre and Lambeth 2010; Heller and Tudzynski 2011).

In mammals, seven members of the NOX family (NOX1–5, DUOX1, and DUOX2) are known (Aguirre *et al.* 2005; Kawahara and Lambeth 2007). The activity of NOX2, the most intensively studied NOX, is regulated by a protein complex containing p22phox, p40phox, p47phox, p67phox, and the small GTPase RAC1. NOX1, NOX3, and NOX4 also require p22phox, whereas the activity of NOX5, DUOX1, and DUOX2 is independent of this regulator (Smith *et al.* 2012). To date, three members of the NOX family are known in fungi. NOX1 and NOX2 [synonymous (syn.) NOXA and NOXB] are homologs of mammalian NOX2 and have been found in most ascomycetes. In contrast, NOX3, the homolog of mammalian NOX5, has been detected only in some fungi like *Aspergillus terreus*, *Magnaporthe grisea*, *Podospora anserina*, and several *Fusarium* species (Aguirre *et al.* 2005; Scott and Eaton 2008; Brun *et al.* 2009). Fungal NOX1 and NOX2 enzymes are regulated by the p67phox homolog NOR1 (NOX regulating, syn. NOXR) and the small GTPase RAC1 (syn. RacA) (Kawahara and Lambeth 2007; Tanaka *et al.* 2008). In *Epichloë festucae*, the putative scaffold protein Bem1 was reported to associate with NOR1 and CDC24 (Takemoto *et al.* 2011). Another candidate NOX regulatory protein is tetraspanin Pls1. Strains from different ascomycetes, lacking the corresponding gene, have phenotypes similar to *nox2* deletion strains (Lambou *et al.* 2008; Ryder *et al.* 2013; Siegmund *et al.* 2013). However, very little is known about the upstream and downstream components of the NOX signaling pathways in fungi.

In this study, we carried out a comprehensive genetic analysis using *S. macrospora* to elucidate the contribution of NOX enzymes to fungal sexual development. In addition to the characterization of sterile mutant pro32, we present a detailed functional analysis of deletion mutants *nox1*, *nox2*, and *nor1* in *S. macrospora*, showing that NOX1 and NOR1 are required for fruiting body development and hyphal fusion. For the first time, we provide RNA-seq analysis of Δnox1 protoperithecia and show NOX1-dependent gene expression compared to gene expression in protoperithecia of the sterile mutant pro1 and wild-type strains. Furthermore, phenotypic and genetic analysis led us to conclude that NOX2 and NOR1 contribute to a signaling pathway controlling ascospore germination and that transcription factor STE12 is part of this pathway. Finally, we relate cAMP levels to NOX2 function. Our analysis extends the current knowledge on the contribution of NOX enzymes to the regulation of two distinct fungal developmental processes and provides important hints to define the cellular routes regulated by these enyzmes.

Materials and Methods

Strains, media, and growth conditions

S. macrospora strains, listed in Table 1, were grown under standard laboratory conditions on complete medium (CM) or cornmeal malt fructification medium (BMM) media (Esser 1982; Nowrousian *et al.* 1999). Cultivation for ascospore germination assays and DNA extraction were performed as described previously (Nowrousian and Cebula 2005; Kamerewerd *et al.* 2008; Teichert *et al.* 2012). For rescue of fertility, strains were inoculated on filter paper covering solid BMM medium. Two consecutive transfers of the filter paper to fresh solid BMM medium were performed after 3 days. Continuous growth on solid BMM medium with or without filter paper served as control (adapted from Malagnac *et al.* 2004). Quantification of linear growth was performed using race tube assays. Recombinant plasmids were propagated in *Escherichia coli* XL1 Blue MRF′ (Stratagene, La Jolla, CA) under standard experimental conditions (Sambrook and Russell 2001).

Preparation of nucleic acids

DNA and RNA were extracted using phenol/chloroform, and RNA was selectively precipitated (Pöggeler *et al.* 1997). For RNA-seq analysis, mycelia were grown in surface cultures for 4 days or directly on slides [Molecular Machines and Industries (MMI)] for fixation and dissection *in situ* (Teichert *et al.* 2012).

Genome sequencing of developmental mutant pro32

Mutant pro32 from our laboratory collection was backcrossed several times with wild type or red-spored fus mutant (Nowrousian *et al.* 2012) and finally crossed with fus. DNA was extracted from 40 sterile and 40 fertile progeny as described previously (Nowrousian *et al.* 2012). Five micrograms of pooled genomic DNA for pro32 and wild type, respectively, was subjected to 50-bp paired-end Illumina/Solexa sequencing with a HiSeq2000 at GATC Biotech (Constance, Germany). Cleaning of raw data, mapping to the *S. macrospora* reference genome, and analysis of sequence variants were performed as previously described (Nowrousian *et al.* 2012). The Burrows Wheeler Alignment tool (Li and Durban 2009) was used for mapping and SAMtools (Li *et al.* 2009) for SNP calling. Further bioinformatics analysis was done using custom-made Perl scripts.

Generation of Δnox1, Δnox2, and Δnor1 deletion strains

Transformation of *S. macrospora* was performed as described previously with an enzyme mix of 1 g VinoTaste Pro (Novozymes, Blagsvaerd, Denmark), 0.3 g Caylase (Cayla, Toulouse, France), and 27 U Chitinase (ASA Spezialenzyme, Wolfenbüttel, Germany) (Walz and Kück 1995; Engh *et al.* 2007). For the generation of transgenic plasmids, homologous recombination in *S. cerevisiae* PJ69-4a and standard cloning procedures were used (James *et al.* 1996; Sambrook and Russell 2001; Colot *et al.* 2006; Bloemendal *et al.* 2012). To allow homologous recombination of *nox* knockout constructs in *S. macrospora* Δku70, the flanking regions of the corresponding *nox* genes together with the *hph* resistance cassette were inserted into pRS426 (Christianson *et al.* 1992). The 5′ and 3′ regions flanking the *nox* genes were amplified

Table 1 ***S. macrospora*** **strains used in this study**

Strain	Relevant genotype	Relevant phenotype	Reference source
S91327	Wild type	F	Culture collection of the Department of General and Molecular Botany
S84595	fus, spore color mutant	F	Culture collection of the Department of General and Molecular Botany
S96888	Δku70::*nat*	F	Pöggeler and Kück (2006)
DD27, DD1	Δnox1::*hph*	S, DG, HFD	This study
DD194, DD299	Δnox2::*hph*/fus	F, GDB	This study
DD118-2	Δnox2::*hph*/Δku70::*nat*	F	This study
DD492, DD574	Δnor1::*hph*/fus	S, GDB, DG, HFD	This study
S104701	Δgsa3::*hph*	F, GD, DG	Kamerewerd *et al.* (2008)
S114583, S114602	Δste12::*hph*/fus	F, GDB	Kamerewerd *et al.* (2008)
S107115	Δgsa3::*hph*/Δnox2::*hph*/fus	F, GD	This study
S83812	Δgsa3::*hph*/Δste12::*hph*/r2	S, DG	Kamerewerd *et al.* (2008)
S144534, S114567	Δnox2::*hph*/Δste12::*hph*/r2	F, GDB	This study
DD1093, DD1161, DD1325	Δnox1::*hph*/*nox1*::*nat*	F, HFD	This study
S106371, S106375, S106755	Δnox2::*hph*/*nox2*::*nat*	F	This study
DD2843, DD2909, DD2958	Δnor1::*hph*/*nor1*::*nat*	F	This study
S69656	Δpro40::*hph*	S	Engh *et al.* (2007)
S109348	pro32	S, HFD	This study
DD291-3-1, DD290-4-3	pro32/*nox1*::*nat*	F	This study

F, fertile; S, sterile; HFD, hyphal fusion defect; GD, germination defect; GDB, germination defect in black ascospores; DG, decreased growth.

with specific oligonucleotides using PCR based on wild-type (S91327) genomic DNA [*nox1*: 5′ region 05007-5fw/05007-5rv (1039 bp), 3′ region 05007-3fw/05007-3rv (1035 bp); *nox2*: 5′ region 08741-5fw/08741-5rv (1065 bp), 3′ region 08741-3fw/08741-3rv (808 bp); *nor1*: 5′ region 02124-5fw/02124-5rv (1064 bp), 3′ region 02124-3fw/02124-3rv (1065 bp)]. The *hph* resistence cassette was obtained from vector pDrivehph (Nowrousian and Cebula 2005) by *Eco*RI restriction. Plasmids pKO-nox1, pKO-nox2, and pKO-nor1 were linearized with restriction enzymes (*Bam*HI, pKO-nox1 and pKO-nor1; *Xho*I, pKO-nox2) and used to transform *S. macrospora* strain Δku70. To verify transformants, genomic DNA was isolated and tested for homologous recombination at the *nox* locus using PCR [Δnox1: 05007_vp1/d1 (1159 bp) and d2/05007_vp2 (2257 bp); Δnox2: 08742_vp1/d1 (1111 bp) and d2/08742_vp2 (1144 bp); Δnor1: 02124_vp1/d1 (1190 bp) and d2/02124_vp2 (1193 bp)]. To verify the deletion of *nox* genes, the following oligonucleotides were used: 05007-5′fw/05007_comp_5′rv (*nox1* 5′ fragment, 2017 bp), 05007_comp_3′fw/05007-3′rv (*nox1* 3′ fragment, 2248 bp), 08741-5′fw/08741_comp_5′rv (*nox2* 5′ fragment, 2053 bp), 08741_comp_3′fw/08741-3′rv (*nox2* 3′ fragment, 1910 bp), 02124-5′fw/02124_comp_5′rv (*nor1* 5′ fragment, 1979 bp), and 02124_comp_3′fw/02124-3′rv (*nor1* 3′ fragment, 1966 bp). Probes for Southern blot detection of *nox* genes were generated by restriction of complementing plasmids (*nox1*: pComp_nox1/*Xho*I; *nox2*: pComp_nox2/*Sph*I; *nor1*: pComp_nor1/*Ksp*I). The *hph* probe was obtained from vector pDrivehph by *Eco*RI restriction (Nowrousian and Cebula 2005).

Plasmids for complementation of *nox* deletion strains were generated as follows: the *nox* ORFs and ~1000 kb up- and downstream regions were amplified via PCR [*nox1*: 05007-5fw/05007-3rv (3889 bp); *nox2*: 08742-5fw/08742-3rv (3709 bp); *nor1*: 02124-5fw/02124-3rv (3842 bp)]. The amplicons were cloned in pRS426_nat (Klix *et al.* 2010) using homologous recombination in yeast. The complementation vectors pComp_nox1, pComp_nox2, and pComp_nor1 were transformed into the corresponding deletion strains. To verify Δnox2 complementation, it was necessary to quantify the ascospore germination of black ascospores. For this, the deletion mutant Δnox2/fus was transformed with pComp_nox2. Resulting strains carrying a *nox2* deletion and an ectopical integration of *nox2* were designated as Δnox2/fus::*nox2*. To obtain black-spored Δnox2::*nox2*, the Δnox2/fus::*nox2* was crossed with wild type, and black ascospores were isolated from recombinant asci. The black-spored Δnox2::*nox2* were verified by PCR. Double deletion strains were obtained via crossing of single deletion mutants followed by the isolation of single spores from recombinant asci as described previously (Esser and Straub 1958). All oligonucleotides and plasmids used in this study are listed in Table 2 and Table 3, respectively.

Microscopy

To investigate sexual propagation, *S. macrospora* was grown on slides with a thin layer of BMM medium at 27° in continuous light (Engh *et al.* 2007). Hyphal fusion assays were performed after 2 days of growth on Sordaria Westergaard's medium overlaid with a cellophane layer (Bio-Rad, München, Germany) (Bloemendal *et al.* 2012). Light microscopy was performed either with an AxioPhot microscope (Zeiss, Jena, Germany) capturing images with an AxioCam using the AxioVision digital system, or AxioImager microscope (Zeiss) capturing images with a Photometrix Cool SnapHQ camera (Roper Scientific). Processing of images was done with MetaMorph (version 7.7.5.0, Universal Imaging) and Adobe

Table 2 Oligonucleotides used in this study

Oligonucleotide	Sequence (5′–3′)	Specificity
05007-5fw	gtaacgccagggttttcccagtcacgacgggatccgaacaaacacaataacaccattgcc	5′ *nox1* with pRS426 overlap; *Bam*HI
05007-5rv	cgagggcaaaggaatagggttccgttgagggttggcgaccgctgaattcctcctc	5′ *nox1* with *hph* overhang
05007-3fw	gcccaaaaatgctccttcaatatcagttgcgttatacttggcttataactataccc	3′ *nox1* with *hph* overlap
05007-3rv	gcggataacaatttcacacaggaaacagcggatcctgattaggcggtattagttatggttg	3′ *nox1* with pRS426 overlap, *Bam*HI
08741-5fw	gtaacgccagggttttcccagtcacgacggtcgacgtccttcggtgatgtgccgagagtgc	5′ *nox2* with pRS426 overlap, *Sal*I
08741-5rv	cgagggcaaaggaatagggttccgttgaggcgtgtctgggttgcttctgttgtcgt	5′ *nox2* with *hph* overlap
08741-3fw	gcccaaaaatgctccttcaatatcagttgcacgtctttgtcggaattcccgttta	3′ *nox2* with *hph* overlap
08741-3rv	gcggataacaatttcacacaggaaacagcgtcgacctttgcggttgtcgctcatgcgatt	3′ *nox2* with pRS426 overlap; *Sal*I
02124-5fw	gtaacgccagggttttcccagtcacgacgggatccctggatacctctaggtcatcaattg	5′ *nor1* with pRS426 overlap, *Bam*HI
02124-5rv	cgagggcaaaggaatagggttccgttgagggttgaggtgttgttagacgtgcgta	5′ *nor1* with *hph* overlap
02124-3fw	gcccaaaaatgctccttcaatatcagttgcaaccagctcgccgtctggttttgg	3′ *nor1* with *hph* overlap
02124-3rv	gcggataacaatttcacacaggaaacagcggatcccgtgaggaagctggttgatcctgag	3′ *nor1* with pRS426 overlap; *Bam*HI
05007_vp1	gccctgaggcgatttttgtttatc	Δnox1
05007_vp2	gcttttcgctctcacggtagattc	Δnox1
d1	cgatggctgtgtagaagtactcgc	*hph*
d2	atccgcctggacgactaaaccaa	*hph*
08741_vp1	ctaagcactttggtccttttcccc	Δnox2
08741_vp2	gattaggaagctgtagatgctcatggag	Δnox2
02124_vp1	ggacaatttccgaggagctggac	Δnor1
02124_vp2	gcttcatgtcagatcgcttgttcc	Δnor1
05007_comp5′rv	gtgccactggtacttggagacttg	*nox1*
05007_comp3′fw	gtatcagacagcaatccttcgaaac	*nox1*
08741_comp5′rv	gttctccttcttgatctggatctcg	*nox2*
08741_comp3′fw	cacatgttcatcgtcttcttcttttttc	*nox2*
02124_comp5′rv	ctatcatccttgacttccagtttcc	*nor1*
02124_comp3′fw	gtgctgaaatcaaaaaatgttagtcttg	*nor1*
5007 cDNA rev	gtgttccttccaaaacctgaaatc	*nox1*
nox1_RT_fw	ggacatggataccacgcaga	*nox1* (qRT-PCR)
nox1_RT_rv	ttccgcatgctctcaaagaa	*nox1* (qRT-PCR)
nor1_RT_fw	ctggtatgcaggatttggca	*nor1* (qRT-PCR)
nor1_RT_rv	gcctcgtttggtcggtagac	*nor1* (qRT-PCR)
nox2_RT_fw_2	ctggttcttttccccgtctg	*nox2* (qRT-PCR)
nox2_RT_rv_2	ggaccatgctgtcgtgatgt	*nox2* (qRT-PCR)
ste12_RT_fw	gcctttcagtcccagtccac	*ste12* (qRT-PCR)
ste12_RT_rv	ctgtcccatgttctgtccca	*ste12* (qRT-PCR)
pro1_RT_fw	ttcgatcgattcgcattttg	*pro1* (qRT-PCR)
pro1_RT_rv	tgatgaatatttgccgctcg	*pro1* (qRT-PCR)
gsa3_RT_fw	tcgaccgaatgagatggatg	*gsa3* (qRT-PCR)
gsa3_RT_rv	cacttcttgcgttcgctacg	*gsa3* (qRT-PCR)
sac1_RT_fw	aggcttgcacttctcttcgg	*sac1* (qRT-PCR)
sac1_RT_rv	ttgagcaggcccgttaatct	*sac1* (qRT-PCR)
smta-1_RT_fw	catcgtcgccgaatacaaga	*Smta-1* (qRT-PCR)
smta-1_RT_rv	aacgacgacactatcgggct	*Smta*-1 (qRT-PCR)
smtA-3_RT_fw	tcatgatgatggaatgggga	*SmtA-3* (qRT-PCR)
smtA-3_RT_rv	ttgttttggcatccgtcttg	*SmtA-3* (qRT-PCR)
smtA-2_RT_fw	agcatgctgcgtcattgagt	*SmtA-2* (qRT-PCR)
smtA-2_RT_rv	cacccaacacatgcacctct	*SmtA-2* (qRT-PCR)
smtA-1_RT_fw	cacgatccctttcacaacga	*SmtA-1* (qRT-PCR)
smtA-1_RT_rv	ggcaagtagttttcgcgacc	*SmtA-1* (qRT-PCR)
SMU6905for	ggcatcacggtcaatggtgt	*teh* (qRT-PCR)
SMU6905rev	tgctcagccatcatcctctca	*teh* (qRT-PCR)
pre1for	gcattcacgcccacatcaac	*pre1* (qRT-PCR)
pre1rev	gttgtgccgaaggtgatgca	*pre1* (qRT-PCR)
pre2for	tccacccgttccataccctg	*pre2* (qRT-PCR)
pre2rev	tcgatgcaagctagttcgcg	*pre2* (qRT-PCR)
ppg1-for	ctccgtgacaccaccttcag	*ppg1* (qRT-PCR)
ppg1-rev	ggaggcatagcgcttcca	*ppg1* (qRT-PCR)
ppg2for	cggtatctcgcctctcaacgt	*ppg2* (qRT-PCR)
ppg2rev	gttgtgctcccattgtgcaga	*ppg2* (qRT-PCR)
tap1_RT_fw	tgaccaagttgcatcccaag	*tap1* (qRT-PCR)
tap1_RT_rv	caaccgtagccctcaacaca	*tap1* (qRT-PCR)
SMU4533Ncofor	ccatggctccctcagtcgatcctaccacc	*app* (Northern blot)
SMU4533Ncorev	ccatggcctccgacggcttgttatcaaccaa	*app* (Northern blot)

Table 3 Plasmids used in this study

Plasmid	Feature	Reference
pRS426	*URA3*, *lacZ_a*, T7_promoter, T3_promoter, *bla*, FRT, *hph*	Christianson *et al.* (1992)
pDrivehph	pDrive with *hph*	Nowrousian and Cebula (2005)
pKO-nox1	pRS426 with 1000 kb 5′ and 3′ region of *nox1*, *hph*	This study
pKO-nox2	pRS426 with kb 5′ and 3′ region of *nox2*, *hph*	This study
pKO-nor1	pRS426 with 1000 kb 5′ and 3′ region of *nor1*, *hph*	This study
pComp-nox1	pRS426 with *nox1* gene and 1000 kb 5′ and 3′, *nat*	This study
pComp-nox2	pRS426 with *nox2* gene and 1000 kb 5′ and 3′, *nat*	This study
pComp-nor1	pRS426 with *nor1* gene and 1000 kb 5′ and 3′, *nat*	This study

Photoshop (Adobe Systems, Dublin, Ireland). The documentation of sexual propagation of complemented strains was done on BMM medium in Petri dishes using a Stemi 2000-C binocular (Zeiss) capturing images with AxioCam ERc5s.

Detection and quantification of ROS

The detection of ROS by nitroblue tetrazolium (NBT) staining was performed as described previously (Malagnac *et al.* 2004) using cultures with mycelia covering the whole plate (grown for 4 days on solid BMM media). This assay was performed with at least three independent biological replicates per strain. Before and 30 min after NBT addition, pictures were taken of all plates with defined camera settings to determine the mean tonal range (Adobe Photoshop, histogram). For every plate the mean tonal range values after the NBT assay were normalized to the values before NBT addition. Resulting values for the mutant strains were then normalized to the corresponding value for the wild type.

Ascospore germination assays

In this study, we used three different ascosopore germination assays. In the first assay, we quantified germination of ascospores discharged from perithecia generated by selfing (ascospore germination assay of selfing strains). For this, fertile strains were cultivated on BMM medium for 5–10 days at 27° in continuous light. When the first discharged ascospores were observed, a Petri dish with thin BMM medium and 0.5% sodium acetate (BMM-Ac) was put upside down on the *S. macrospora* culture to directly catch discharged ascospores. After 5 hr incubation at 27°, a minimum of 500 ascospores were microscopically analyzed for germination.

In our second ascospore germination assay, we investigated the effect of different concentrations of ascorbate (antioxidant) and cAMP on germinating ascospores using cell permeable N^6, 2′-O-dibutyryl-cAMP (db-cAMP, BioLog). In this assay, we used the fertile wild-type and fus strains, which were cultivated and analyzed as described for the ascospore germination assay of selfing strains, except that ascospores were discharged on BMM-Ac medium supplemented with different concentrations of db-cAMP or ascorbate.

To investigate the influence of a certain gene deletion on ascospore germination in sterile mutants, we performed an ascospore germination assay as a crossing experiment (crossing ascospore germination assay). All the investigated strains carried the *fus* mutation and were crossed with wild type (black ascospores), leading to recombinant asci containing black and red ascospores. After 11 days, wild type (black) and fus (red) ascospores were isolated from recombinant perithecia and recovered on BMM-Ac medium. Colonies from at least 100 germinated black (wild type) and 100 germinated red (fus) spores were tested for hygromycin B resistance to detect those carrying a gene deletion.

RNA-seq analysis

For RNA-seq analysis, RNA isolated from wild-type and Δnox1 mycelia and protoperithecia was used. For protoperithecia isolation by laser microdissection (LM), the Δnox1 mutant was grown directly on slides for fixation and dissection *in situ* (Teichert *et al.* 2012). RNA was isolated from protoperithecia with the Arcturus PicoPure kit (Applied Biosystems, Carlsbad, CA) and amplified in two linear amplification rounds using the TargetAmp 2-Round aRNA Amplification kit 2.0 (Epicentre Biotechnologies, Madison, WI) with modifications as described in Teichert *et al.* (2012). For RNA isolation of total mycelia, strains were precultured for 2 days on solid BMM. From these plates, three 20-ml BMM liquid cultures were inoculated and incubated for an additional 4 days. RNA from mycelia was isolated using phenol/chloroform extraction. RNA from protoperithecia (3.5 μg) and total mycelia (400 μg) was used for library preparation and Illumina/Solexa sequencing at GATC Biotech. cDNA libraries were prepared with the TrueSeq RNA sample preparation kit (Illumina, San Diego, CA) and sequenced with a HiSeq2000. For wild-type total mycelia, RNA from one sample was sequenced, for Δnox1 mycelia and Δnox1 protoperithecia, RNA from two independent biological replicates was used for sequencing. Resulting reads were cleaned and mapped to the reference *S. macrospora* genome v2 (Teichert *et al.* 2012). Differential expression was evaluated using DESeq (Anders and Huber 2010) and a method called "classical analysis." In this analysis, genes were grouped into five groups (0 to 4) containing genes that are not differentially expressed (group 0) to genes that are strongly and significantly differentially expressed (group 4) as described in Teichert *et al.* (2012). Based on the DESseq and classical analysis, a consensus was calculated according to the following criteria for differential expression similar to what was described before (Teichert *et al.* 2012): a gene is described as differentially regulated if ratios in both DESeq and classical analysis are >4 or <0.25, DESeq adjusted P-value ≤ 0.1, and a gene in groups 1–4 in

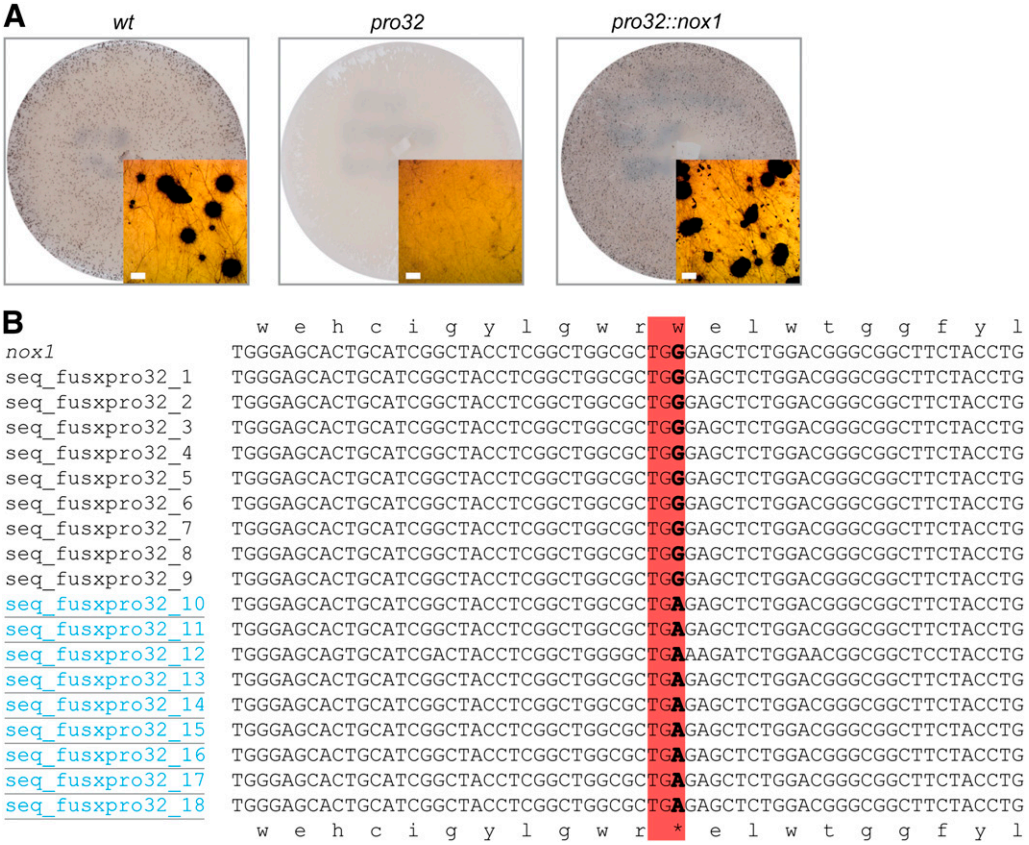

Figure 1 Genome sequencing of pro32 mutants reveals a mutation in the *nox1* gene. (A) Sexual phenotypes of indicated strains. Insets show a detailed view of either wild-type black perithecia or mutant light brown protoperithecia. Bar, 100 μm. (B) Sequence comparison of the *nox1* gene from wild type and 18 ascospore isolates from a cross between pro32 and fus strains. Sterile strains (underlined and blue) show a G to A transition, which changes *nox1* W222 codon to a TGA stop codon (boxed).

the classical analysis. For comparisons of mycelia *vs.* protoperithecia samples, ratio thresholds were set to >8 and <0.125 (Supporting Information, File S1).

Quantitative real-time PCR

Quantitative real-time PCR (qRT-PCR) was performed as described previously (Nowrousian *et al.* 2005) using the master mix from the Promega GoTaq qPCR kit for SybrGreen. qRT-PCR was performed in a StepOnePlus (Applied Biosystems) using StepOne software v2.2. Sequences of oligonucleotides used are given in Table 2.

Accession numbers

Raw sequence data from sequencing mutant pro32 (pro32/fus) and wild type (wt_3) were submitted to the National Center for Biotechnology Information (NCBI) sequence read archive (accession no. SRP033637). The RNA-seq reads and derived expression ratios were submitted to the Gene Expression Omnibus (GEO) database (accession no. GSE49363).

Results

Genome sequencing of mutant pro32 identifies a point mutation in nox1 encoding NADPH oxidase 1

We have previously generated a collection of sterile pro mutants with a developmental block after protoperithecia formation (Kück *et al.* 2009). Using next-generation sequencing for efficient and time-saving identification of mutations (Nowrousian *et al.* 2012), we sequenced the genome of sterile pro32 (Figure 1A). After cleaning of raw sequence data from pro32 and a wild-type reference strain, the majority of reads (>95%) mapped to the reference genome (Table S1). We identified one mutation with 100% penetrance at position 810 of *SMAC_05007* encoding a putative NADPH oxidase 1 (NOX1) in pro32, but not in the wild-type sample (Table 4). The point mutation in pro32 results in a transition from G to A at position 810 of the *SMAC_05007* ORF, creating an early stop codon. As a consequence, the highly conserved NOX1 ferredoxin reductase-like C-terminal domain is missing from the NOX1 protein of the mutant strain (Figure S1). After crossing of pro32 to spore color mutant fus that carries a mutation in the *tih* melanin biosynthesis gene (Nowrousian *et al.* 2012), PCR fragments covering the *nox1* gene were obtained from nine fertile and nine sterile ascospore progeny. Sequencing of PCR fragments confirmed the *nox1* base pair substitution in all strains with the sterile pro32 phenotype (Figure 1B). NOX1 function in fruiting body development was further verified by transformation of pro32 with a wild-type *nox1* gene including 5′ and 3′ flanking regions. The resulting transformants showed a restoration of fertility, as indicated by the formation of mature fruiting bodies (Figure 1A).

Deletion mutants lacking nox1 or nor1 show developmental defects

To further investigate NOX1 function in *S. macrospora*, we generated deletion mutants of *nox1* as well as *nor1* (*SMAC_02124*),

Table 4 Summary of small sequence variants detected in the pro32 genome when compared to the reference genome

Genotype	Sequence sample	No. of small variants with coverage >40%	No. of mutations with 100% penetrance	Location of putative mutations
wt	wt_3	146	—	—
pro32	pro32/fus	142	3	G810A in *SMAC_05007* results in stop codon at W222 C926T in *SMAC_05015* does not result in change of amino acid sequence C2620T in *SMAC_05015* results in V310I

Mutations caused by small sequence variants were identified by screening the sequence data for SNPs and indels (insertions/deletions) of <4 bases with a coverage of at least 40% of the average coverage for that sample. For these putative mutations, it was subsequently checked whether they had 100% penetrance, *i.e.*, all the reads in the strain had the SNP/indel and none of the reads in the sequenced wild-type sample carried this specific mutation.

which encodes the NOX regulator NOR1. These genes show 89 and 94% similarity to the corresponding genes from *Neurospora crassa* (accession nos. XP_964104 and XM_958018, respectively). The *nox1* and *nor1* genes were replaced by the hygromycin B resistance cassette through homologous recombination at the 5′ and 3′ regions flanking the target genes in a Δku70 host (Figure S2). The transformants were crossed with fus, a mutant generating red ascospores, to obtain homokaryotic strains carrying the *nox1* or *nor1* deletions without the *ku70* deletion. Correct replacement of *nox1* or *nor1* with the *hph* cassette was verified by Southern hybridization using *hph*-, *nox1*-, or *nor1*-specific probes (Figure S3).

Δnox1 and Δnor1 mutants showed distinctive similar phenotypes when compared to the wild-type strain. Both mutants have a sterile phenotype, being able to generate protoperithecia, but no perithecia (Figure 2A). As shown in Figure 2B, microscopic investigations revealed that both strains, as well as the pro32 mutant, are defective in vegetative cell fusion. In addition, Δnox1 and Δnor1 mutants were characterized by a significant reduction in hyphal growth by ∼61 and 21%, respectively (Figure 2C). With these phenotypes, pro32, Δnox1, and Δnor1 resemble other pro mutants found in a screen to detect strains having a developmental block after protoperithecia formation (Kück *et al.* 2009). To complement Δnox1 and Δnor1 mutants, we transformed them with full-length copies of *nox1* or *nor1* genes. In all cases, the reduced growth and sterility phenotypes were rescued in the transformants. However, hyphal fusion was only observed in the Δnor1::*nor1* and pro32::*nox1* strains, but not in Δnox1::*nox1* (Figure S4). Further, the ectopic integration of *nox1* in the corresponding deletion mutant leads only to a reduced number of perithecia, suggesting dose-dependent effects in the Δnox1::*nox1* complemented strain. Nevertheless, complementation analysis of Δnor1 and pro32 prove that functional *nox1* and *nor1* genes are required for vegetative cell fusion, hyphal growth, and proper fruiting body formation.

For *P. anserina*, it has been shown that the fertility defect of a *PanoxA* deletion mutant is rescued by serial transfers of the fungus to nutrient-rich medium (Malagnac *et al.* 2004). We observed a similar rescue of the *S. macrospora nox1* deletion mutant (Figure S5). After germination of Δnox1 ascospores from the rescued strain, we again obtained sterile strains that showed only protoperithecia formation. To determine whether this rescue phenotype is a general feature of sterile pro mutants, we performed serial media shifts using Δnor1 and the unrelated Δpro40 mutant (Figure S5). In contrast to Δnox1, these mutants remained sterile even after several transfers.

Hyphal fusion mutants show elevated levels of ROS

NADPH oxidases are known to produce ROS in a highly spatiotemporally regulated fashion (Aguirre and Lambeth 2010). Using the NBT assay for the detection of superoxide, we quantified the level of ROS in pro32, Δnox1, and Δnor1, as well as in other mutant strains affected in perithecia development and/or defective in hyphal fusion. Compared to wild type, sterile and hyphal fusion defective pro32, Δnox1, and Δnor1 showed enhanced ROS levels in vegetative hyphae (Figure 3A) and protoperithecia (Figure 3B). This enhancement of ROS is also shared by the hyphal fusion mutant Δpro40 (Engh *et al.* 2007). In contrast, all investigated mutants with wild-type-like cell fusion showed wild-type-like levels of ROS. As a consequence of the hyphal fusion defect in Δnox1 and other developmental mutants, we propose conditional nutrient starvation, and thus sterility in these strains.

In protoperithecia, NOX1 regulates transcription of genes for hyphal fusion and cytoskeleton remodeling

To obtain information about differentially regulated genes that are dependent on NOX1 activity, we performed RNA-seq analysis using RNA samples obtained from wild-type and Δnox1 mycelia and protoperithecia (Table S2). Mycelia were isolated from surface liquid cultures, while protoperithecia samples were obtained using a recently developed laser microdissection technique that allows protoperithecia isolation with minimal mycelial contamination (Teichert *et al.* 2012).

To allow conclusions about gene expression in protoperithecia of different developmental mutants, we included RNA-seq data obtained in a previous study for protoperithecia of the wild-type and the sterile mutant pro1 (File S1) (Teichert *et al.* 2012). *pro1* encodes C_6 zinc finger transcription factor PRO1 (Masloff *et al.* 1999) and shares the sterile phenotype with Δnox1 strains. Comparison of

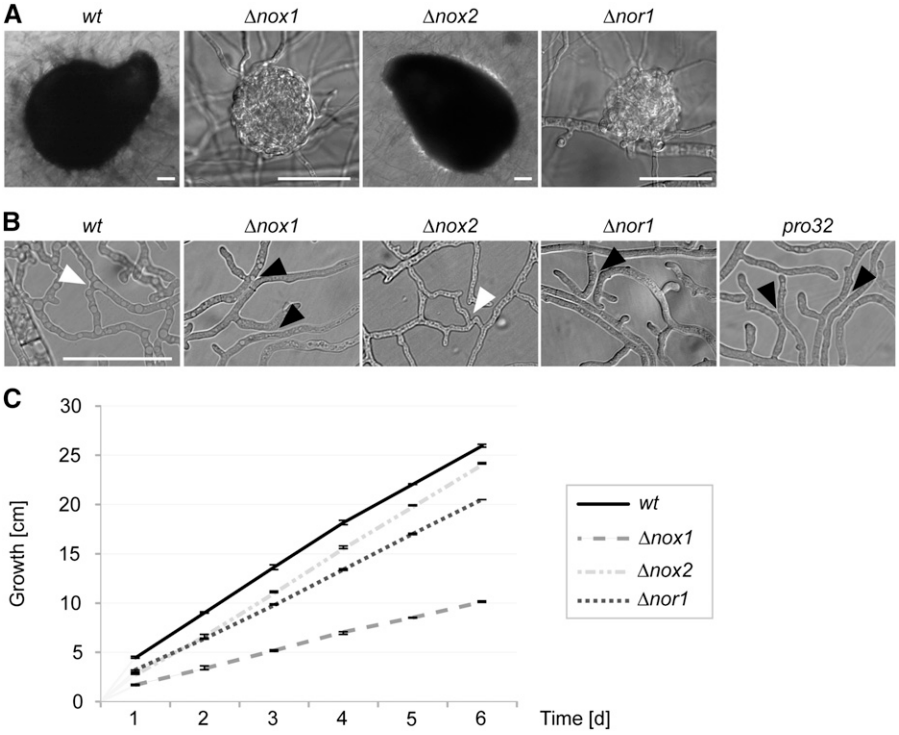

Figure 2 Phenotype of *nox* and *nor1* deletion mutants. (A) Strains Δnox1 and Δnor1 are unable to develop black perithecia, and thus produce only slightly pigmented protoperithecia. Mutant Δnox2 shows wild-type-like sexual development. Pictures were taken after 7 days of growth on BMM medium and incubation at 27° in constant light. Bar, 50 μm. (B) Δnox1, pro32, and Δnor1, but not Δnox2, are affected in hyphal fusion. Strains were grown for 2 days on minimal medium on a cellophane layer in 27° in constant light. The assay was performed at least three times for every mutant. Hyphal fusion is indicated by white arrowheads; the lack of hyphal fusion between hyphae in close contact is marked by black arrowheads. Bar, 50 μm. (C) Δnox1 and Δnor1, but not Δnox2 mutants, show decreased linear growth. Growth was followed in race tubes for 6 days in three replicates.

genome-wide expression patterns between the different samples (total mycelia from wild type and Δnox1 as well as protoperithecia from wild type, Δnox1, and pro1) showed that the protoperithecial samples cluster apart from the mycelial samples, and that Δnox1 protoperithecia are more similar to pro1 protoperithecia than to wild-type protoperithecia (Figure S6A). This reinforces a previous finding that expression patterns of protoperithecia are distinct from those of nonreproductive mycelia (Teichert *et al.* 2012). Furthermore, the fact that pro1 and Δnox1 protoperithecia cluster together indicates that there is a common mutant-specific expression pattern in young fruiting bodies blocked at a similar developmental stage. These findings were confirmed by a comparison of differentially expressed genes in protoperithecia and mycelial samples (Figure 4A) and an analysis of the 500 most strongly expressed genes in each of the samples ("top500" analysis, Figure S6B). A total of 501 genes are differentially expressed in both, Δnox1 and pro1 protoperithecia, compared to wild-type protoperithecia, whereas only 33 genes are differentially expressed specifically in the comparison of Δnox1 and wild-type protoperithecia as well as Δnox1 and wild-type mycelia (Figure 4A). The top500 analysis showed that intersections between wild-type and Δnox1 mycelia and intersections between the protoperithecial samples contained more genes than intersections between protoperithecial and mycelial samples (Figure S6B).

To identify the possible functions of genes differentially regulated in Δnox1 compared to wild-type protoperithecia, we performed functional categories (FunCat, $P < 0.05$) and BLAST analyses, using the *N. crassa* orthologs for FunCat analysis. Figure 4B illustrates functional categories (FunCat) for all *N. crassa* orthologs, in total 554 up- (red) and 432 down-regulated (blue) genes. Significantly overrepresented categories correspond to metabolism and cell rescue (down-regulated compared to wild type), as well as cell cycle and protein synthesis (up-regulated compared to wild type).

Furthermore, BLAST analysis of differentially regulated genes in Δnox1 protoperithecia revealed that several of these genes encode proteins important for cytoskeleton remodeling, like CDC42, profilin, cofilin, and coronin-1 (Table S3). Coronin-1 has been shown to have a major role in actin organization and dynamics in *N. crassa* (Echauri-Espinosa *et al.* 2012). In a second group, genes important for hyphal fusion are differentially regulated in Δnox1 protoperithecia compared to wild-type protoperithecia. Among these is the *ham-10* gene, which is essential for hyphal fusion and perithecia formation in *N. crassa* (Fu *et al.* 2011) (Table S3, Table S4). The third group contains genes encoding subunits of NADH:oxidoreductases of the respiratory chain and of mitochondrial ATPase. Consistent with this, mutants unable to assemble the respiratory chain complex I are female sterile in *N. crassa* (Duarte and Videira 2000) (Table S3, Table S4). The enrichment of these three groups together with the FunCat analysis suggests that NOX1 has regulatory functions, *e.g.*, in cytoskeleton remodeling, hyphal fusion, metabolism, and mitochondrial respiration.

Extensive genetic analysis has identified a large number of developmental genes involved in fruiting body formation (Pöggeler *et al.* 2006; Kück *et al.* 2009; Engh *et al.* 2010).

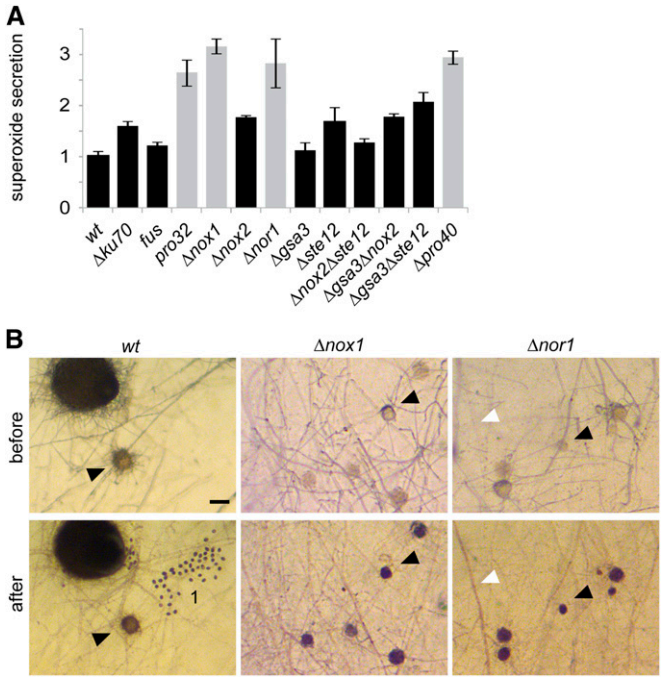

Figure 3 Mutants affected in hyphal fusion show increased levels of NBT reduction. (A) Quantitative measurement (fold change) of NBT precipitates after 30 min of incubation in at least three replicates. Gray bars indicate hyphal fusion-deficient strains. Hyphal fusion defect correlates with sterility, except for sterile mutant Δgsa3Δste12, which can undergo normal hyphal fusion. Normalization was done in reference to wild type. (B) Detailed view of sexual (black arrowheads) and vegetative (white arrowheads) structures stained by NBT. Bar, 50 μm, 1 = ascospores.

Results from the RNA-seq-based differential expression analysis of these genes are given in Table 5. In Figure 4C results from qRT-PCR analysis are shown to verify some of the results of the RNA-seq analysis, and to further compare gene expression patterns in mycelia and protoperithecia from Δnox1 and other developmental mutants. RNA-seq data show that both pheromone receptor genes *pre1* and *pre2* and the two mating type genes *SmtA-1* and *SmtA-3* are up-regulated in Δnox1 mycelia and protoperithecia. Similarly, genes for melanin biosynthesis (*pks*, *teh*, *sdh*, and *tih*) and two genes associated with fruiting body maturation, *app* and *tap1*, are down-regulated in Δnox1 mycelia and protoperithecia, similar to the situation in other pro mutants (Nowrousian *et al.* 2005, 2007; Teichert *et al.* 2012), whereas they only show minor expression changes in fertile mutants Δnox2 and Δste12 compared to wild type (Figure 4C). These findings are in line with the proposed hypothesis of a common pro mutant-specific expression pattern.

NOX2 is required for the germination of melanized ascospores

Like other ascomycetes, the genome of *S. macrospora* encodes a second NADPH oxidase, NOX2. The corresponding *nox2* gene (*SMAC_08741*) shows 91% sequence similarity to its *N. crassa* homolog (accession no. XP_001728356). A homokaryotic Δnox2/fus strain was generated with the strategy described in *Materials and Methods*. As can be seen in Figure 2, this strain has no defect in vegetative growth, cell fusion, or sexual development. However, when we performed random ascospore analysis from a cross of the primary transformant Δku70Δnox2 with the melanin-deficient fus mutant, we observed in a total of 390 analyzed viable ascospores a strict cosegregation of the hygromycin-B-resistant phenotype, corresponding to the *nox2* deletion, with fus. To investigate ascospore germination further, we tested germination of diverse fertile strains generating either black or red spores. For sound statistical analysis, we investigated a minimum of 400 spores in each of three replicate experiments and tested their germination capacity on solid BMM-Ac medium. We analyzed wild type, fus, and the Δku70 strain, the latter of which was used as the recipient strain for generating the Δnox2 mutant. As can be seen in Figure 5A, ascospores generally showed a germination rate between 40 and 70%. Similar results were obtained with the red-spored Δnox2/fus strain. However, we were unable to isolate any viable (germinating) ascospores from black-spored Δku70/Δnox2 mutants, indicating that germination in Δnox2 is suppressed by the presence of melanin.

To verify the strict dependence of the germination defect on melanization, we generated a black-spored Δnox2::*nox2* complemented strain. Primary transformant Δku70Δnox2 was not appropriate for complementation experiments since it carries selection markers *nat1* (noursethricin resistance) and *hph* (hygromycin B resistance) replacing *ku70* and *nox2*, respectively. Therefore, we transformed hygromycin-resistant Δnox2/fus with a wild-type copy of *nox2*. The red-spored Δnox2/fus::*nox2* was then crossed to wild type, and black ascospores were isolated carrying the Δnox2 deletion and the ectopically integrated *nox2* gene. Three randomly selected strains germinated at a frequency similar to wild type and Δku70 (Figure 5A), confirming that germination of black ascospores is strictly dependent on NOX2 function.

To assess whether the germination defect is restricted to Δnox2, we tested further the ascospore germination phenotype of Δnox1 and Δnor1, both having a sterile phenotype. Δnox1/fus and Δnor1/fus double mutants were crossed to the wild type, and the germination assays of black and red spores were done as described in *Materials and Methods*. As can be seen from Table 6, Δnor1, but not Δnox1 ascospores, displayed the same melanin-dependent germination defect as Δnox2 ascospores. This result indicates that NOR1 is required to regulate both NOX1 and NOX2.

These data suggest that ROS is necessary for spore germination. It might be hypothesized that in the wild type, both NOX2 as well as other pathways contribute to ROS production allowing spore germination. The Δnox2 mutant would then retain residual amounts of ROS generated independently of NOX2; however, the residual

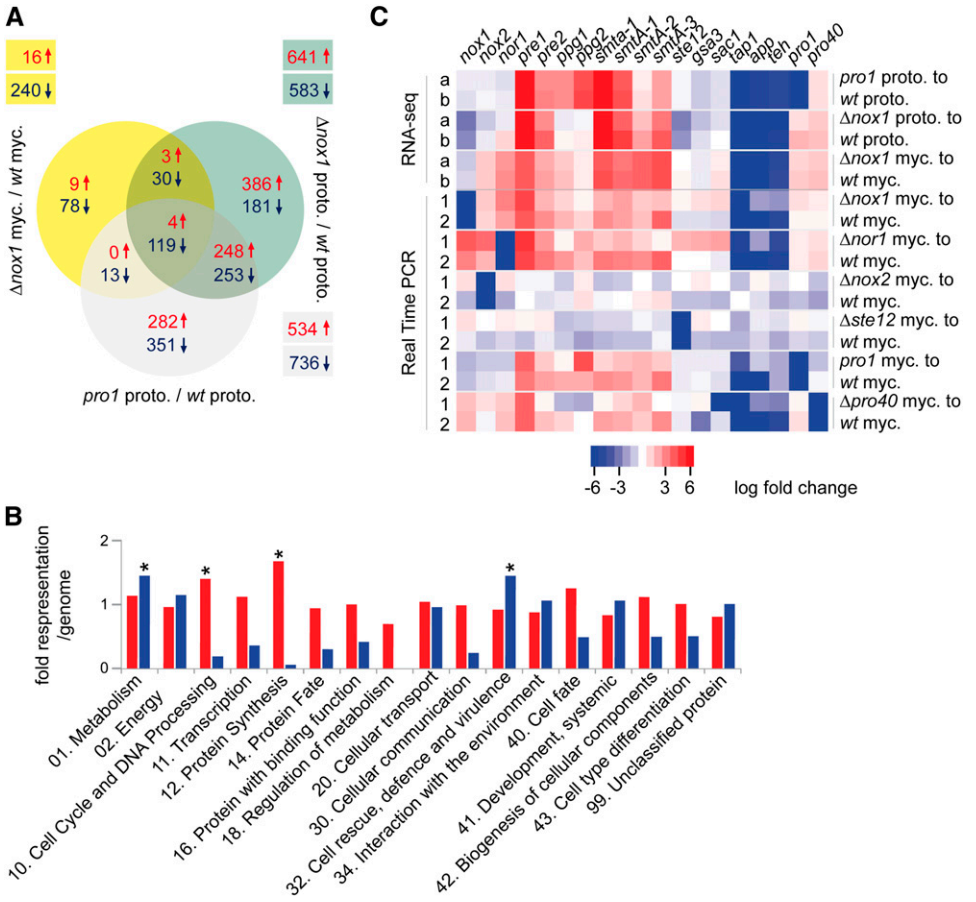

Figure 4 Results of RNA-seq-based expression analysis in developmental mutants. (A) Consensus analysis of differentially regulated genes identified by DESeq and classical statistical methods. Differentially regulated genes in relation to the corresponding wild-type tissue are indicated in yellow (Δnox1 mycelia), green (Δnox1 protoperithecia), and gray (pro1 protoperithecia). The numbers of up- (↑, red) and down- (↓, blue) regulated genes are indicated. (B) Illustration of functional categories (FunCat) (Ruepp *et al.* 2004) of up- (red) and down- (blue) regulated genes in protoperithecia from Δnox1 mutant compared to wild-type protoperithecia. For each FunCat category, the fold representation compared to its representation among all predicted proteins is given. Asterisks indicate statistically overrepresented functional groups (*P*-value ≤ 0.05). (C) Heatmap of regulated genes in RNA-seq and qRT-PCR experiments using RNA from protoperithecia (proto.) and mycelium (myc.). Different statistical analyses are indicated by "a" (DESeq) and "b" (classical). Numbers (1 and 2) indicate biological replicates. Up- (red) and down- (blue) regulated genes are indicated.

amount of ROS in Δnox2 ascospores might be scavenged by melanin in black ascospores. To further test this hypothesis, we performed germination tests with different ascorbate concentrations in the germination media. Ascorbate is an antioxidant that scavenges ROS. As can be seen in Figure 5B, germination of ascospores on ascorbate-containing media is drastically reduced in strains lacking *nox2* in the fus mutant background but less pronounced in the fus reference strain. Thus, the antioxidant ascorbate mimics the effect of melanin in Δnox2/fus spores.

NOX2, NOR1, and transcription factor STE12 act in a genetic pathway determining ascospore germination

The melanin-dependent ascospore germination defect of Δnox2 and Δnor1 prompted us to look for other genes involved in this process. Previously, *S. macrospora* deletion mutants lacking the *gsa3* (alpha subunit 3 of the heterotrimeric G-protein), *sac1* (adenylate cyclase), and *ste12* genes were shown to have an ascospore germination defect (Nolting and Pöggeler 2006; Kamerewerd *et al.* 2008). We performed further crossing experiments to test whether these genes act with *nox2* and *nor1* in the same genetic pathway. Δgsa3/fus, Δsac1/fus, and Δste12/fus were crossed to a wild-type strain and then 100 black and 100 red germinating ascospores from these crosses were tested for hygromycin B resistance. As can be seen in Table 6, the *ste12* deletion, but not the *gsa3* or *sac1* deletions, strictly cosegregated with the *fus* mutation. Thus, the germination defect of Δste12 resembles the Δnox2 and Δnor1 ascospore germination defect. To further verify this result, we generated triple mutant Δnox2Δste12/fus, having a fertile phenotype (Figure 5C). From a cross of the triple mutant with wild type, we isolated a total of 146 ascospores. Of these, 68 were red colored and hygromycin B resistant, thus indicating the deletion of *nox2* and/or *ste12*. In contrast, 78 black and red ascospores showed wild-type-like sensitivity to hygromycin B. These data thus verify the strict cosegregation of the *nox2* or *ste12* deletion with the *fus* mutation, indicating that NOX2 and STE12 act in the same pathway that controls ascospore germination.

In contrast to Δnox2, Δnor1, and Δste12, *sac1* and *gsa3* deletion mutants have a germination defect that is independent of melanin in ascospores (Table 6). To determine whether the *gsa3* and the *nox2* pathways overlap, we generated triple mutant Δgsa3Δnox2/fus. Like the single deletion strains, this strain is fertile (Figure 5C); however, the ascospores are unable to generate germination vesicles in contrast to the control strains fus and Δnox2/fus. Instead, they burst after ~5 hr on germination medium (Figure 5D, File S2, File S3, File S4). None of the 4000 ascospores analyzed showed germination.

Table 5 Log_2 ratios of relative expression of known developmental genes in Δnox1 mycelium and protoperithecia

		Log_2 ratios of gene expression in mycelium of Δnox1 *vs.* wt		Log_2 ratios of gene expression in protoperithecia of Δnox1 *vs.* wt	
S. macrospora locus tag	Gene	DESeq analysis	Classical analysis	DESeq analysis	Classical analysis
		Transcription factor genes			
SMAC_00338	*pro1*	1.011	1.295	0.955	1.787
SMAC_03223	*pro44*	−0.358	−0.140	−2.059	−1.380
SMAC_05219	*mcm1*	−0.041	0.081	−1.296	−0.565
SMAC_06479	*ste12*	0.050	0.330	−2.836	−2.196
		Pheromone pathway genes			
SMAC_02283	*pre1*	3.907	4.041	7.720	7.381
SMAC_08994	*pre2*	2.104	2.231	2.867	3.631
SMAC_05970	*ppg1*	1.434	1.446	−0.365	0.320
SMAC_12697	*ppg2*	0.496	0.540	−0.166	0.583
		Mating type genes			
SMAC_05404	*Smta-1*	4.052	4.188	[a]	[a]
SMAC_05401	*SmtA-1*	3.331	3.366	3.750	4.562
SMAC_05402	*SmtA-2*	3.836	3.827	1.440	2.207
SMAC_05403	*SmtA-3*	4.295	4.303	3.162	3.862
		Nox genes			
SMAC_05007	*nox1*	−1.109[b]	−0.913[b]	−3.076[b]	−2.404[b]
SMAC_08741	*nox2*	1.210	1.430	−1.006	−0.299
SMAC_02124	*nor1*	2.532	2.718	−0.376	1.025
		MAP kinase cell integrity pathway genes			
SMAC_03673	*mik1*	0.479	0.717	1.284	1.939
SMAC_02183	*mek1*	0.813	0.967	0.401	1.033
SMAC_05504	*mak1*	0.546	0.743	−1.545	−0.870
		STRIPAK complex genes			
SMAC_08794	*pro11*	0.255	0.474	1.400	2.050
SMAC_02580	*pro22*	0.230	0.417	−0.985	−0.273
SMAC_00877	*mob3*	−0.245	−0.084	0.311	0.988
SMAC_01224	*pro45*	0.372	0.601	−0.210	0.438
SMAC_01919	*pp2AA*	0.876	0.95	1.152	1.841
SMAC_04678	*pp2Ac1*	1.234	1.305	1.173	1.827
		Melanin biosynthesis genes			
SMAC_03130	*pks*	−4.541	−4.251	−6.916	−6.057
SMAC_05880	*teh*	−4.829	−4.679	−6.227	−5.523
SMAC_02101	*sdh*	−3.656	−3.603	−4.134	−2.870
SMAC_05650	*tih*	−5.819	−5.601	−7.691	−6.990
		G-protein alpha subunit genes			
SMAC_05328	*gsa1*	−0.094	0.120	−0.360	0.311
SMAC_06605	*gsa2*	0.235	0.386	−0.422	0.220
SMAC_07195	*gsa3*	−0.453	−0.311	−1.325	−0.682
		Genes associated with ascospore germination			
SMAC_01638	*sac1*	0.714	0.825	−0.619	0.037
SMAC_09071	*rac1*	0.235	0.393	0.875	1.729
		Genes associated with fruiting body maturation			
SMAC_06095	*app*	−8.505	−8.274	−7.069	−6.419
SMAC_03372	*tap1*	−8.984	−8.722	−9.364	−8.716
SMAC_00522	*fbm1*	1.470	1.810	0.181	1.150
		Other essential genes for fruiting body development			
SMAC_07802	*pro4*	2.579	2.901	0.536	1.347
SMAC_04848	*pro41*	2.354	2.511	0.406	1.110
SMAC_06775	*acl1*	−1.353	−1.174	−0.734	0.100
SMAC_08608	*asf1*	0.879	0.988	1.141	1.809
SMAC_06539	*atg7*	−0.355	−0.233	−0.643	0.041
SMAC_04815	*pro40*	1.225	1.468	1.225	1.468

[a] No reads mapped in wild-type protoperithecia. Therefore no ratios can be calculated.
[b] Counted reads map to 5′ and 3′ UTRs of *nox1*, which were not deleted in the Δnox1 mutant.

Thus, the germination-related phenotypes of Δnox2 and Δgsa3 (Kamerewerd *et al.* 2008) are exacerbated in the Δgsa3Δnox2/fus mutant. This result clearly shows that NOX2 and GSA3 have a different impact on ascospore germination. Therefore, we propose that ascospore germination is regulated by two pathways, namely the NOX2-NOR1-STE12 and the GSA3-SAC1 pathways (Figure 6).

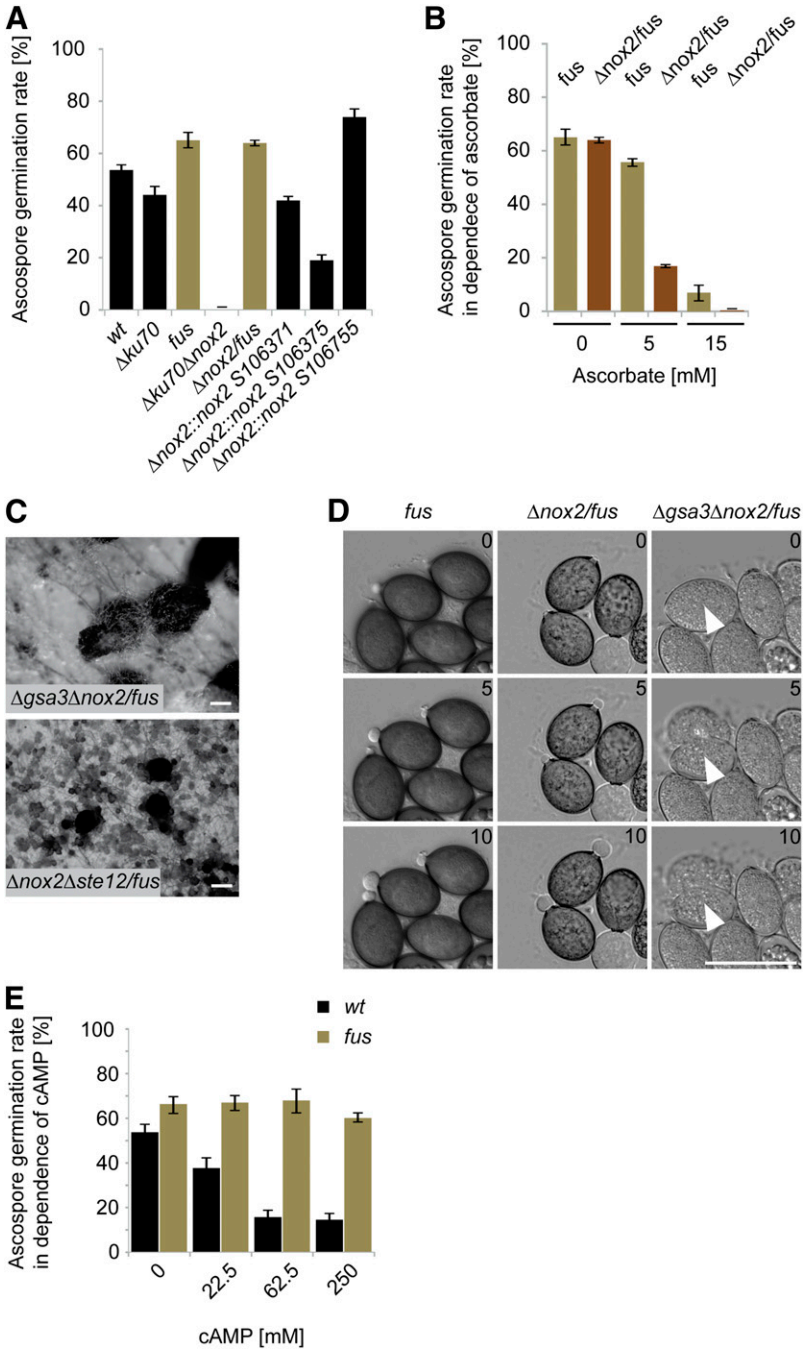

Figure 5 Phenotypes of ascospore germination-defective mutants. (A) Quantification of germination of ascospores discharged from selfed perithecia from wild type, different mutants, and Δnox2::*nox2* strains. A minimum of 400 ascospores per strain were tested in each of three biological replicates. Black bars represent strains with full melanized ascospores; brown bars represent strains with a block in melanin biosynthesis. (B) Ascospore germination under different ascorbate concentrations. A minimum of 400 ascospores from selfed perithecia were tested for each strain and ascorbate concentration. (C) Perithecia formation of Δgsa3Δnox2/fus and Δnox2Δste12/fus mutants after 7 and 14 days incubation, respectively. Bar, 100 μm. (D) Time series of ascospore germination for the indicated mutants. The elapsed time in minutes is indicated. White arrowheads mark ascospores that burst instead of showing a germinaton vesicle. Bar, 50 μm. (E) Wild-type and fus mutant ascospore germination rates in the presence of db-cAMP. Discharged ascospores were collected and incubated on medium containing the indicated db-cAMP concentrations. A minimum of 400 ascospores per strain were tested for each of three biological replicates. Black bars represent strains with full melanized ascospores; brown bars represent strains with a block in melanin biosynthesis.

cAMP inhibits germination of melanized ascospores

Recent reports indicate that cAMP, generated by an adenylate cyclase homologous to SAC1, inhibits the activity of a NOX2 homolog in human cells (Diebold *et al.* 2009; Li *et al.* 2012). At the molecular level, ROS production by the mammalian NOX2 complex is proposed to be reduced when the NOX2 activator RAC1 is directly inhibited by high cAMP concentrations. In analogy to this model, we hypothesized that increased cAMP levels could inhibit NOX2 activity in *S. macrospora* and reduce ascospore germination. To test this hypothesis, discharged ascospores from wild-type and fus strains were germinated on BMM-Ac medium supplemented with different concentrations of cell-permeable db-cAMP (Figure 5E). A concentration of 22.5 mM db-cAMP resulted in a reduction of ascospore germination of ~30% in the wild type, but not in the red-spored fus mutant, which does not require NOX2 activity for germination. At higher db-cAMP concentrations of 62.5 mM and 250 mM, ascospore germination frequency of wild type, but not fus, dropped down by 70%. Thus, cAMP is able to mimic the ascospore germination defect of Δnox2, Δnor1, and Δste12 in a concentration-dependent manner. Based on these results, we hypothesize that cAMP generated by the GSA3-SAC1 pathway (Kamerewerd *et al.* 2008) exerts a negative

Table 6 Frequency of hygromycin B resistance in black- and red-spored progeny from indicated crosses

	100 germinated black ascospores		100 germinated red ascospores	
Cross	Hyg^S	Hyg^R	Hyg^S	Hyg^R
Δnox1/fus × wt	65	35	49	51
Δnox2/fus × wt	100	0	43	57
Δnor1/fus × wt	100	0	48	52
Δgsa3/fus × wt	92	8	81	19
Δsac1/fus × wt	80	20	81	19
Δste12/fus × wt	100	0	47	53
Δpro40/fus × wt	45	55	43	57

From each cross, 100 black and 100 red colony forming ascospores were tested for hygromycin B resistance, indicating the deletion of the corresponding gene.

regulatory role on NOX2 activity, which results in decreased production of ROS and failure to establish an ascospore germination vesicle, thus connecting the *nox2/ste12* and *gsa3/sac1* pathways (Figure 6).

Discussion

Fruiting body development is regulated by NOX1 and NOR1

The deletion of *nox1* and *nor1* genes led to a sterile phenotype that has been found previously in a set of *S. macrospora* developmental pro mutants, which can form protoperithecia, but are hampered in developing mature fruiting bodies (Kück *et al.* 2009). The deletion of *nox1* or *nor1* in other filamentous fungi leads to similar effects on sexual development. In *Aspergillus nidulans*, *noxA* deletion blocks the differentiation of cleistothecia (Lara-Ortiz *et al.* 2003), and similarly, *P. anserina* and *N. crassa nox1* mutants are female sterile (Malagnac *et al.* 2004; Cano-Dominguez *et al.* 2008). Notably, in *P. anserina* (Malagnac *et al.* 2004) and *S. macrospora*, the sterile phenotype can be rescued by serially shifting the mutant to rich medium, indicating that sterility is related to the availability of nutritional factors, or ROS scavenging and signaling molecules. Alternatively, shifts to rich medium might induce the activity of NOX2, thereby bypassing the *nox1* deletion.

A novel function of NOX1 and NOR1 was recently detected in *N. crassa* and *Botrytis cinerea* (Read *et al.* 2012; Roca *et al.* 2012), where a deletion of the corresponding genes abolishes fusion of conidial anastomosis tubes (CATs). *S. macrospora* does not form any conidia; however, hyphal fusion can be observed within the hyphal network (Rech *et al.* 2007). Our investigation showed that *S. macrospora nox1* and *nor1* mutants have a defect in hyphal fusion, as was also shown for corresponding mutants from *E. festucae* (Kayano *et al.* 2013). Both phenomena, sterility and hyphal fusion defect, are correlated but not strictly linked with each other. For example, the *N. crassa ham-4* mutant is fertile but shows a hyphal fusion defect (Simonin *et al.* 2010) and the sterile *Smatg8* mutant from *S. macrospora* still shows hyphal fusion (Voigt and Pöggeler 2013).

Since NOX enzymes are known to produce superoxide by the reduction of oxygen (Leto *et al.* 2009), we determined the levels of ROS using the NBT assay. Interestingly, we detected higher superoxide levels in all mutants tested that were defective in hyphal fusion, including Δpro40. The superoxide level has been investigated in *nox* deletion mutants of several ascomycetes and diverging results have emerged. For example, while *E. festucae nox1* mutants show decreased superoxide levels (Tanaka *et al.* 2008), increased levels of superoxide are detected in corresponding mutants of *M. oryzae*, *P. anserina*, and *B. cinerea* (Malagnac *et al.* 2004; Egan *et al.* 2007; Siegmund *et al.* 2013). The latter results are rather unexpected since NOX enzymes are known to generate superoxide. Nevertheless, our results highlight that not only a deletion of the *nox1* gene leads to elevated superoxide levels, but also a deletion of *pro40*. Thus, our data support a general correlation between a hyphal fusion defect and enhanced superoxide levels generated by a yet unknown source in mutant strains, as was proposed previously (Malagnac *et al.* 2004; Egan *et al.* 2007; Siegmund *et al.* 2013).

Transcriptional profiling reveals differentially regulated genes in a nox1 mutant

Recently, transcriptional profiling of mycelia from a *P. anserina Panox1* mutant was performed by microarray analysis and showed the deregulation of a large set of genes involved in carbohydrate degradation and secondary metabolism (Bidard *et al.* 2012). However, the authors analyzed total mycelia after 72 hr of growth, therefore expression patterns specific to sexual structures could not be elucidated in these experiments. Thus, our RNA-seq analysis of protoperithecia as well as mycelia significantly extends the current knowledge about NOX1-dependent gene expression by including sexual structures from a specific developmental stage. The increased levels of ROS in the Δnox1 mutant might also be responsible for some of the gene expression changes observed.

One finding was that a large set of genes involved in cytoskeleton remodeling and hyphal fusion is differentially regulated in the Δnox1 mutant. This finding is consistent with recent studies in *Magnaporthe oryzae*, where the NOX1

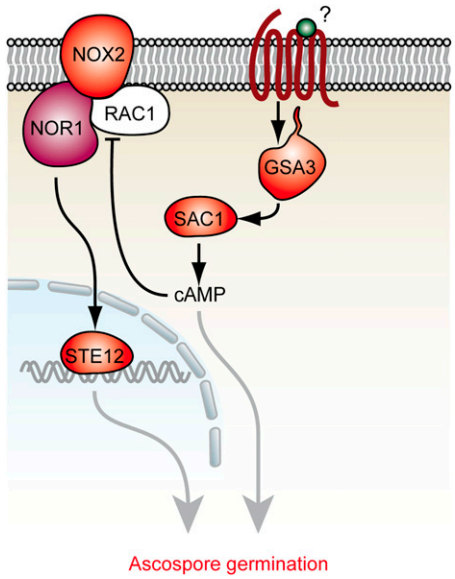

Figure 6 Interplay of two pathways regulating ascospore germination in *S. macrospora*. During ascospore germination, two different signaling pathways, NOX2-NOR1-STE12 and GSA3-SAC1, exist and may be interconnected by cAMP. Work from other studies indicates that the GTPase RAC1 is inhibited by cAMP and thus negatively regulates the NOX2-NOR1 complex (Diebold *et al.* 2009).

complex was shown to be important for the maintenance of the cortical F-actin network during penetration of the host plant (Ryder *et al.* 2013). These authors showed that Δnox1 still initated penetration peg formation but was unable to proliferate in the infected plant tissue. Furthermore, Yno1p, the NOX enzyme from yeast, has a regulatory role in actin remodeling (Rinnerthaler *et al.* 2012). Interestingly, F-actin remodeling is also crucial for CAT fusion in *N. crassa* (Roca *et al.* 2010). Further, our RNA-seq analysis revealed that among the differentially expressed genes in Δnox1 protoperithecia, there are some involved in the establishment of hyphal polarity. For example, *cdc42*, a gene central for the establishment of polarity, is up-regulated in Δnox1 protoperithecia compared to wild-type protoperithecia. The activity of CDC42 is regulated by the guanine nucleotide exchange factor (GEF) CDC24 and the scaffold protein BEM1, both of which are able to interact with the NOR1 homolog of *E. festucae* in a yeast-two-hybrid assay (Takemoto *et al.* 2011). In *N. crassa*, Bem1 is actively recruited around the forming fusion pore of germlings, and *bem1* deletion leads to a drastic reduction of germling fusion, indicating a cross-talk between polarity establishment and hyphal fusion (Schürg *et al.* 2012). In *N. crassa* it was further shown that Δcdc24 and Δcdc42 are fusion defective (Read *et al.* 2012). Taken together, our results support a model in which the differential expression of a set of genes involved in cytoskeleton remodeling and hyphal fusion is responsible for the inability of Δnox1 mutants to undergo cell fusion, normal polar growth, and perithecia development. The regulated genes are prime candidates for further analysis of NOX1-dependent developmental functions.

Besides NOX enzymes, there are other ROS-producing enzymes and processes within a cell, among them complex I of the respiratory chain that includes NADH:oxidoreductases (Murphy 2009). Our RNA-seq data indicate the up-regulation of subunits of the respiratory chain NADH:oxidoreductase of complex I and Cytochrome c in Δnox1, whereas two ATPase subunits are down-regulated. Thus, we propose that the enhanced ROS levels observed in Δnox1 may be due to de-regulation of the mitochondrial respiratory chain, perhaps as a consequence of starvation of hyphae and protoperithecia. This would be consistent with the finding that a serial transfer to fresh media restores fertility of the Δnox1 mutant strain (Figure S5). A similar phenomenon has been described for multiple human cell lines (Scherz-Shouval and Elazar 2007; Chen and Gibson 2008). There, starvation leads to an up-regulation of mitochondrial ROS, which in turn directly activates an autophagy-inducing pathway (Li *et al.* 2013).

NOX2, NOR1, and STE12 act in a genetic pathway controlling ascospore germination

Our results show that NOX2 and NOR1 are required for the germination of sexual spores. Similar defects have been observed in corresponding *P. anserina* (Malagnac *et al.* 2004) and *N. crassa* (Cano-Dominguez *et al.* 2008) mutants. We found that NOX2 is required for germination of melanized ascospores only, since melanin-deficient ascospores from Δnox2 are able to germinate. Lambou *et al.* (2008) suggested for *P. anserina* that the weakened cell wall of pigment-deficient ascospores and the absence of melanin either triggered the germination process or prevented its inhibition. However, the ROS scavenging capacity of melanin (Riley 1997) might also play a role in this process. We propose that ROS is necessary for spore germination and a residual amount in Δnox2 ascospores is scavenged by melanin, thus preventing germination. On the other hand, such residual ROS would not be scavenged in pigment-deficient ascospores, allowing ascospores to germinate.

The ascospore germination assays provided the novel finding that NOX2, NOR1, and the transcription factor STE12 might act in the same genetic pathway to regulate ascospore germination, while SAC1 and GSA3 act in a parallel but interconnected pathway. Indeed, the inhibitory effect of cAMP on germination of melanized ascospores suggests a link between both pathways. In human cells, an increased level of cAMP inhibits GTPase RAC1, which itself is required for NOX2 activity (Diebold *et al.* 2009). We propose that cAMP generated by adenylate cyclase SAC1 inhibits NOX2 activity via the RAC1 homolog (SMAC_09071) (Figure 6). The fact that *gsa3* and *sac1* deletion mutants are fertile suggests that cAMP might not play an important role in NOX1 regulation during growth and perithecia development. In summary, our analyses of ascospore germination in various mutants show that two genetic pathways, NOX2-NOR1-STE12 and GSA3-SAC1, are involved in the regulatory network governing this process.

Acknowledgments

We are grateful to Susanne Schlewinski, Swenja Ellßel, Ingeborg Godehardt, and Regina Ricke for their excellent technical assistance. We also thank Kathrin Grieß for help with some of the experiments. This work was funded by the Deutsche Forschungsgemeinschaft (Bonn-Bad Godesberg) through Forschergruppe FOR 1334, DFG Grant NO407/4-1, and DFG-CONACYT Germany–México Collaboration Grant 75306.

Literature Cited

Aguirre, J., M. Rios-Momberg, D. Hewitt, and W. Hansberg, 2005 Reactive oxygen species and development in microbial eukaryotes. Trends Microbiol. 13: 111–118.

Aguirre, J., and J. D. Lambeth, 2010 Nox enzymes from fungus to fly to fish and what they tell us about Nox function in mammals. Free Radic. Biol. Med. 49: 1342–1353.

Anders, S., and W. Huber, 2010 Differential expression analysis for sequence count data. Genome Biol. 11: R106.

Bidard, F., E. Coppin, and P. Silar, 2012 The transcriptional response to the inactivation of the PaMpk1 and PaMpk2 MAP kinase pathways in *Podospora anserina*. Fungal Genet. Biol. 49: 643–652.

Bloemendal, S., Y. Bernhards, K. Bartho, A. Dettmann, O. Voigt *et al.*, 2012 A homologue of the human STRIPAK complex controls sexual development in fungi. Mol. Microbiol. 84: 310–323.

Brun, S., F. Malagnac, F. Bidard, H. Lalucque, and P. Silar, 2009 Functions and regulation of the Nox family in the filamentous fungus *Podospora anserina*: a new role in cellulose degradation. Mol. Microbiol. 74: 480–496.

Cano-Dominguez, N., K. Alvarez-Delfin, W. Hansberg, and J. Aguirre, 2008 NADPH oxidases NOX-1 and NOX-2 require the regulatory subunit NOR-1 to control cell differentiation and growth in *Neurospora crassa*. Eukaryot. Cell 7: 1352–1361.

Chen, Y., and S. B. Gibson, 2008 Is mitochondrial generation of reactive oxygen species a trigger for autophagy? Autophagy 4: 246–248.

Christianson, T. W., R. S. Sikorski, M. Dante, J. H. Shero, and P. Hieter, 1992 Multifunctional yeast high-copy-number shuttle vectors. Gene 110: 119–122.

Colot, H. V., G. Park, G. E. Turner, C. Ringelberg, C. M. Crew *et al.*, 2006 A high-throughput gene knockout procedure for *Neurospora* reveals functions for multiple transcription factors. Proc. Natl. Acad. Sci. USA 103: 10352–10357.

Diebold, I., T. Djordjevic, A. Petry, A. Hatzelmann, H. Tenor *et al.*, 2009 Phosphodiesterase 2 mediates redox-sensitive endothelial cell proliferation and angiogenesis by thrombin via Rac1 and NADPH oxidase 2. Circ. Res. 104: 1169–1177.

Duarte, M., and A. Videira, 2000 Respiratory chain complex I is essential for sexual development in Neurospora and binding of iron sulfur clusters are required for enzyme assembly. Genetics 156: 607–615.

Echauri-Espinosa, R. O., O. A. Callejas-Negrete, R. W. Roberson, S. Bartnicki-Garcia, and R. R. Mourino-Perez, 2012 Coronin is a component of the endocytic collar of hyphae of *Neurospora crassa* and is necessary for normal growth and morphogenesis. PLoS ONE 7: e38237.

Egan, M. J., Z. Y. Wang, M. A. Jones, N. Smirnoff, and N. J. Talbot, 2007 Generation of reactive oxygen species by fungal NADPH oxidases is required for rice blast disease. Proc. Natl. Acad. Sci. USA 104: 11772–11777.

Engh, I., C. Würtz, K. Witzel-Schlomp, H. Y. Zhang, B. Hoff *et al.*, 2007 The WW domain protein PRO40 is required for fungal fertility and associates with Woronin bodies. Eukaryot. Cell 6: 831–843.

Engh, I., M. Nowrousian, and U. Kück, 2010 *Sordaria macrospora*, a model organism to study fungal cellular development. Eur. J. Cell Biol. 89: 864–872.

Esser, K., 1982 *Cryptogams-Cyanobacteria*, *Algae*, *Fungi*, *Lichens*, Cambridge University Press, London.

Esser, K., and J. Straub, 1958 Genetic studies on *Sordaria macrospora* Auersw., compensation and induction in gene-dependent developmental defects. Z. Vererbungsl. 89: 729–746.

Fu, C., P. Iyer, A. Herkal, J. Abdullah, A. Stout *et al.*, 2011 Identification and characterization of genes required for cell-to-cell fusion in *Neurospora crassa*. Eukaryot. Cell 10: 1100–1109.

Halliwell, B., and J. M. C. Gutteridge, 2007 *Free Radicals in Biology and Medicine*, Oxford University Press, Oxford.

Heller, J., and P. Tudzynski, 2011 Reactive oxygen species in phytopathogenic fungi: signaling, development, and disease. Annu. Rev. Phytopathol. 49: 369–390.

James, P., J. Halladay, and E. A. Craig, 1996 Genomic libraries and a host strain designed for highly efficient two-hybrid selection in yeast. Genetics 144: 1425–1436.

Kamerewerd, J., M. Jansson, M. Nowrousian, S. Pöggeler, and U. Kück, 2008 Three alpha-subunits of heterotrimeric G proteins and an adenylyl cyclase have distinct roles in fruiting body development in the homothallic fungus *Sordaria macrospora*. Genetics 180: 191–206.

Kawahara, T., and J. D. Lambeth, 2007 Molecular evolution of *Phox*-related regulatory subunits for NADPH oxidase enzymes. BMC Evol. Biol. 7: 178.

Kayano, Y., A. Tanaka, F. Akano, B. Scott, and D. Takemoto, 2013 Differential roles of NADPH oxidases and associated regulators in polarized growth, conidiation and hyphal fusion in the symbiotic fungus *Epichloë festucae*. Fungal Genet. Biol. 56: 87–97.

Klix, V., M. Nowrousian, C. Ringelberg, J. J. Loros, J. C. Dunlap *et al.*, 2010 Functional characterization of *MAT1–1*-specific mating-type genes in the homothallic ascomycete *Sordaria macrospora* provides new insights into essential and nonessential sexual regulators. Eukaryot. Cell 9: 894–905.

Kück, U., S. Pöggeler, M. Nowrousian, N. Nolting, and I. Engh, 2009 *Sordaria macrospora*, a model system for fungal development, pp. 17–39 in *The Mycota XV: Physiology and Genetics*, edited by T. Anke, and D. Weber. Springer, Berlin.

Lambeth, J. D., 2004 NOX enzymes and the biology of reactive oxygen. Nat. Rev. Immunol. 4: 181–189.

Lambou, K., F. Malagnac, C. Barbisan, D. Tharreau, M. H. Lebrun *et al.*, 2008 The crucial role of the Pls1 tetraspanin during ascospore germination in *Podospora anserina* provides an example of the convergent evolution of morphogenetic processes in fungal plant pathogens and saprobes. Eukaryot. Cell 7: 1809–1818.

Lara-Ortiz, T., H. Riveros-Rosas, and J. Aguirre, 2003 Reactive oxygen species generated by microbial NADPH oxidase NoxA regulate sexual development in *Aspergillus nidulans*. Mol. Microbiol. 50: 1241–1255.

Leto, T. L., S. Morand, D. Hurt, and T. Ueyama, 2009 Targeting and regulation of reactive oxygen species generation by Nox family NADPH oxidases. Antioxid. Redox Signal. 11: 2607–2619.

Li, H., and R. Durban, 2009 Fast and accurate short read alignment with Burrows-Wheeler Transform. Bioinformatics 25: 1754–1760.

Li, H., B. Handsaker, A. Wysoker, T. Fennell, J. Ruan *et al.*, 2009 The Sequence Alignment/Map format and SAMtools. Bioinformatics 25: 2078–2079.

Li, L., Y. Chen, and S. B. Gibson, 2013 Starvation-induced autophagy is regulated by mitochondrial reactive oxygen species leading to AMPK activation. Cell. Signal. 25: 50–65.

Li, N., B. Li, T. Brun, C. Deffert-Delbouille, Z. Mahiout *et al.*, 2012 NADPH oxidase NOX2 defines a new antagonistic role

for reactive oxygen species and cAMP/PKA in the regulation of insulin secretion. Diabetes 61: 2842–2850.
Malagnac, F., H. Lalucque, G. Lepere, and P. Silar, 2004 Two NADPH oxidase isoforms are required for sexual reproduction and ascospore germination in the filamentous fungus Podospora anserina. Fungal Genet. Biol. 41: 982–997.
Masloff, S., S. Pöggeler, and U. Kück, 1999 The *pro1*$^{+}$ gene from *Sordaria macrospora* encodes a C_6 zinc finger transcription factor required for fruiting body development. Genetics 152: 191–199.
Murphy, M. P., 2009 How mitochondria produce reactive oxygen species. Biochem. J. 417: 1–13.
Nolting, N., and S. Pöggeler, 2006 A STE12 homologue of the homothallic ascomycete *Sordaria macrospora* interacts with the MADS box protein MCM1 and is required for ascosporogenesis. Mol. Microbiol. 62: 853–868.
Nowrousian, M., and P. Cebula, 2005 The gene for a lectin-like protein is transcriptionally activated during sexual development, but is not essential for fruiting body formation in the filamentous fungus *Sordaria macrospora*. BMC Microbiol. 5: 64.
Nowrousian, M., S. Masloff, S. Pöggeler, and U. Kück, 1999 Cell differentiation during sexual development of the fungus *Sordaria macrospora* requires ATP citrate lyase activity. Mol. Cell. Biol. 19: 450–460.
Nowrousian, M., C. Ringelberg, J. C. Dunlap, J. J. Loros, and U. Kück, 2005 Cross-species microarray hybridization to identify developmentally regulated genes in the filamentous fungus *Sordaria macrospora*. Mol. Genet. Genomics 273: 137–149.
Nowrousian, M., M. Piotrowski, and U. Kück, 2007 Multiple layers of temporal and spatial control regulate accumulation of the fruiting body-specific protein APP in *Sordaria macrospora* and *Neurospora crassa*. Fungal Genet. Biol. 44: 602–614.
Nowrousian, M., I. Teichert, S. Masloff, and U. Kück, 2012 Whole-genome sequencing of *Sordaria macrospora* mutants identifies developmental genes. G3 2: 261–270.
Pöggeler, S., and U. Kück, 2006 Highly efficient generation of signal transduction knockout mutants using a fungal strain deficient in the mammalian *ku70* ortholog. Gene 378: 1–10.
Pöggeler, S., S. Risch, U. Kück, and H. D. Osiewacz, 1997 Mating-type genes from the homothallic fungus *Sordaria macrospora* are functionally expressed in a heterothallic ascomycete. Genetics 147: 567–580.
Pöggeler, S., M. Nowrousian, and U. Kück, 2006 Fruiting body development in ascomycetes, pp. 325–355 in *The Mycota I: Growth, Differentiation and Sexuality*, edited by U. Kües, and R. Fischer. Springer, Berlin.
Read, N. D., A. B. Goryachev, and A. Lichius, 2012 The mechanisitc basic of self-fusion between conidial anastomosis tubes during fungal colony initiation. Fungal Biol. Rev. 26: 1–11.
Rech, C., I. Engh, and U. Kück, 2007 Detection of hyphal fusion in filamentous fungi using differently fluorescence-labeled histones. Curr. Genet. 52: 259–266.
Riley, P. A., 1997 Melanin. Int. J. Biochem. Cell Biol. 29: 1235–1239.
Rinnerthaler, M., S. Buttner, P. Laun, G. Heeren, T. K. Felder *et al.*, 2012 Yno1p/Aim14p, a NADPH-oxidase ortholog, controls extramitochondrial reactive oxygen species generation, apoptosis, and actin cable formation in yeast. Proc. Natl. Acad. Sci. USA 109: 8658–8663.
Roca, M. G., H. C. Kuo, A. Lichius, M. Freitag, and N. D. Read, 2010 Nuclear dynamics, mitosis, and the cytoskeleton during the early stages of colony initiation in *Neurospora crassa*. Eukaryot. Cell 9: 1171–1183.
Roca, M. G., M. Weichert, U. Siegmund, P. Tudzynski, and A. Fleissner, 2012 Germling fusion via conidial anastomosis tubes in the grey mould *Botrytis cinerea* requires NADPH oxidase activity. Fungal. Biol. 116: 379–387.
Ruepp, A., A. Zollner, D. Maier, K. Albermann, J. Hani *et al.*, 2004 The FunCat, a functional annotation scheme for systematic classification of proteins from whole genomes. Nucleic Acids Res. 32: 5539–5545.
Ryder, L. S., Y. F. Dagdas, T. A. Mentlak, M. J. Kershaw, C. R. Thornton *et al.*, 2013 NADPH oxidases regulate septin-mediated cytoskeletal remodeling during plant infection by the rice blast fungus. Proc. Natl. Acad. Sci. USA 110: 3179–3184.
Sambrook, J., and D. W. Russell, 2001 *Laboratory Cloning: A Laboratory Manual*, Cold Spring Harbor Laboratory Press, Cold Spring Harbor, NY.
Scherz-Shouval, R., and Z. Elazar, 2007 ROS, mitochondria and the regulation of autophagy. Trends Cell Biol. 17: 422–427.
Schürg, T., U. Brandt, C. Adis, and A. Fleissner, 2012 The *Saccharomyces cerevisiae* BEM1 homologue in *Neurospora crassa* promotes co-ordinated cell behaviour resulting in cell fusion. Mol. Microbiol. 86: 349–366.
Scott, B., and C. J. Eaton, 2008 Role of reactive oxygen species in fungal cellular differentiations. Curr. Opin. Microbiol. 11: 488–493.
Siegmund, U., J. Heller, J. A. L. van Kan, and P. Tudzynski, 2013 The NADPH oxidase complexes in *Botrytis cinerea*: evidence for a close association with the ER and the tetraspanin Pls1. PLoS ONE 8: e55879.
Simonin, A. R., C. G. Rasmussen, M. Yang, and N. L. Glass, 2010 Genes encoding a striatin-like protein (*ham-3*) and a forkhead associated protein (*ham-4*) are required for hyphal fusion in *Neurospora crassa*. Fungal Genet. Biol. 47: 855–868.
Smith, S. M., J. Min, T. Ganesh, B. Diebold, T. Kawahara *et al.*, 2012 Ebselen and congeners inhibit NADPH oxidase 2-dependent superoxide generation by interrupting the binding of regulatory subunits. Chem. Biol. 19: 752–763.
Takemoto, D., S. Kamakura, S. Saikia, Y. Becker, R. Wrenn *et al.*, 2011 Polarity proteins Bem1 and Cdc24 are components of the filamentous fungal NADPH oxidase complex. Proc. Natl. Acad. Sci. USA 108: 2861–2866.
Tanaka, A., D. Takemoto, G. S. Hyon, P. Park, and B. Scott, 2008 NoxA activation by the small GTPase RacA is required to maintain a mutualistic symbiotic association between *Epichloë festucae* and perennial ryegrass. Mol. Microbiol. 68: 1165–1178.
Teichert, I., G. Wolff, U. Kück, and M. Nowrousian, 2012 Combining laser microdissection and RNA-seq to chart the transcriptional landscape of fungal development. BMC Genomics 13: 511.
Voigt, O., and S. Pöggeler, 2013 Autophagy genes *Smatg8* and *Smatg4* are required for fruiting-body development, vegetative growth and ascospore germination in the filamentous ascomycete *Sordaria macrospora*. Autophagy 9: 33–49.
Walz, M., and U. Kück, 1995 Transformation of *Sordaria macrospora* to hygromycin B resistance: characterization of transformants by electrophoretic karyotyping and tetrad analysis. Curr. Genet. 29: 88–95.

Communicating editor: J. Heitman

GENETICS

Supporting Information
http://www.genetics.org/lookup/suppl/doi:10.1534/genetics.113.159368/-/DC1

New Insights Into the Roles of NADPH Oxidases in Sexual Development and Ascospore Germination in *Sordaria macrospora*

Daniela Elisabeth Dirschnabel, Minou Nowrousian, Nallely Cano-Domínguez, Jesus Aguirre, Ines Teichert, and Ulrich Kück

DOI: 10.1534/genetics.113.159368

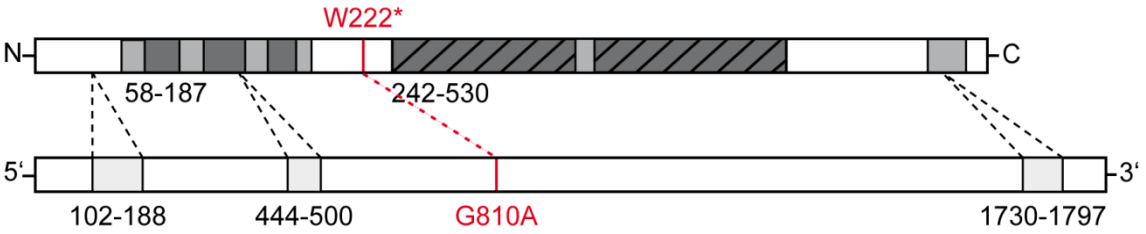

Figure S1 Structure of the *nox1* gene and derived protein. The 1874 bp gene contains three introns (light grey boxes) and the predicted mature mRNA encodes a protein of 645 aa, containing a highly conserved ferric recuctase-like domain at the N-terminus (dark grey boxes), a ferredoxin reductase like domain (striped dark grew boxes) and six predicted transmembrane domains (light grey boxes). A G810A mutation in sterile mutant pro32 leads to a translational stop at position 222 of the NOX1 protein, resulting in a severely truncated NOX1 lacking the ferredoxin reductase-like domain.

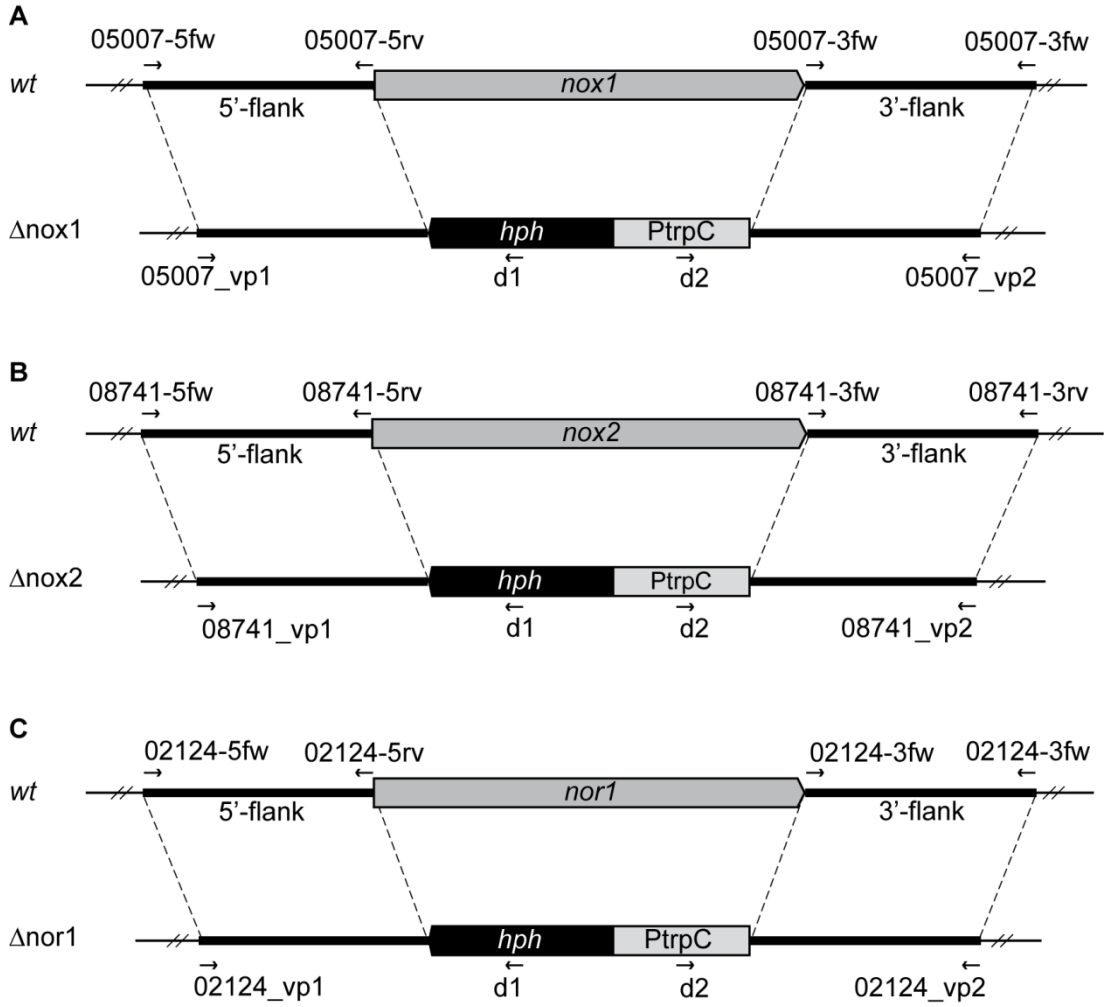

Figure S2 Genomic organization of *nox1* (A), *nox2* (B) and *nor1* (C) loci in wild type and deletion mutants. Primers used for PCR (Table 2) are indicated with small arrows.

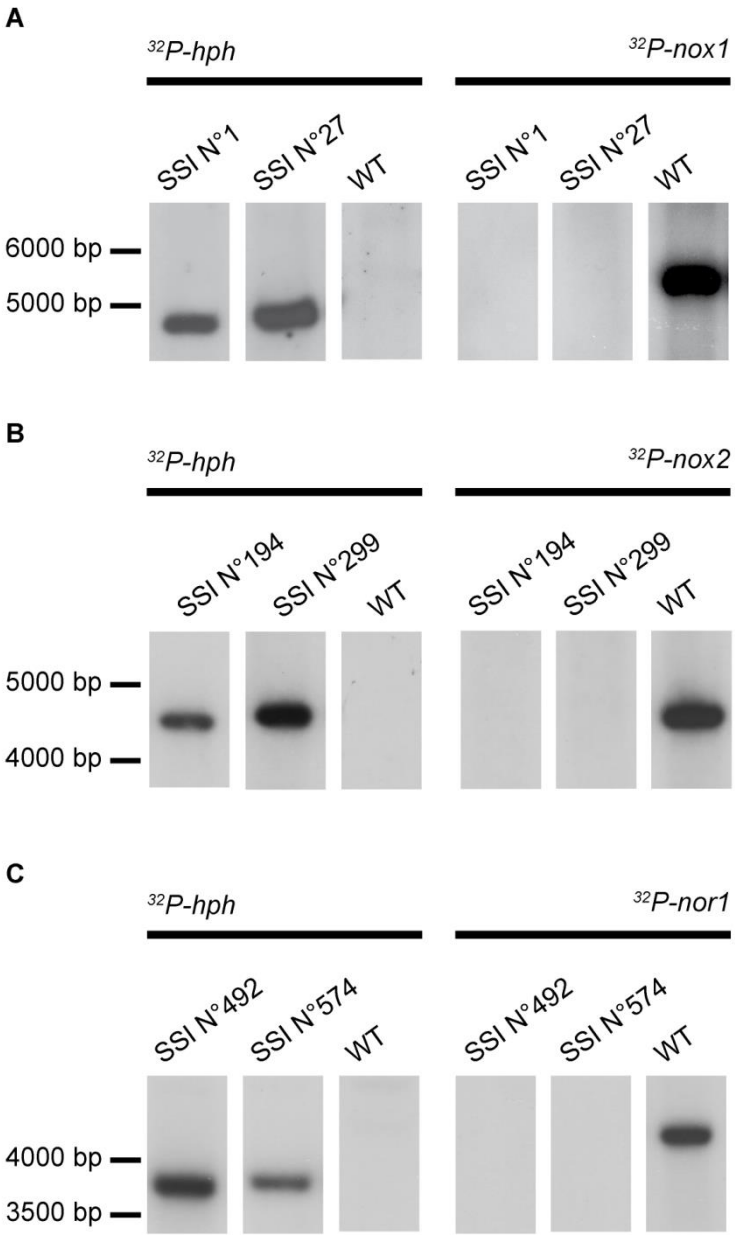

Figure S3 Southern hybridisation of single spore isolates (SSI) to verify the deletion of *nox1* (A), *nox2* (B) and *nor1* (C) mutants. Samples were hybridized with *hph* or gene-specific probes as indicated.

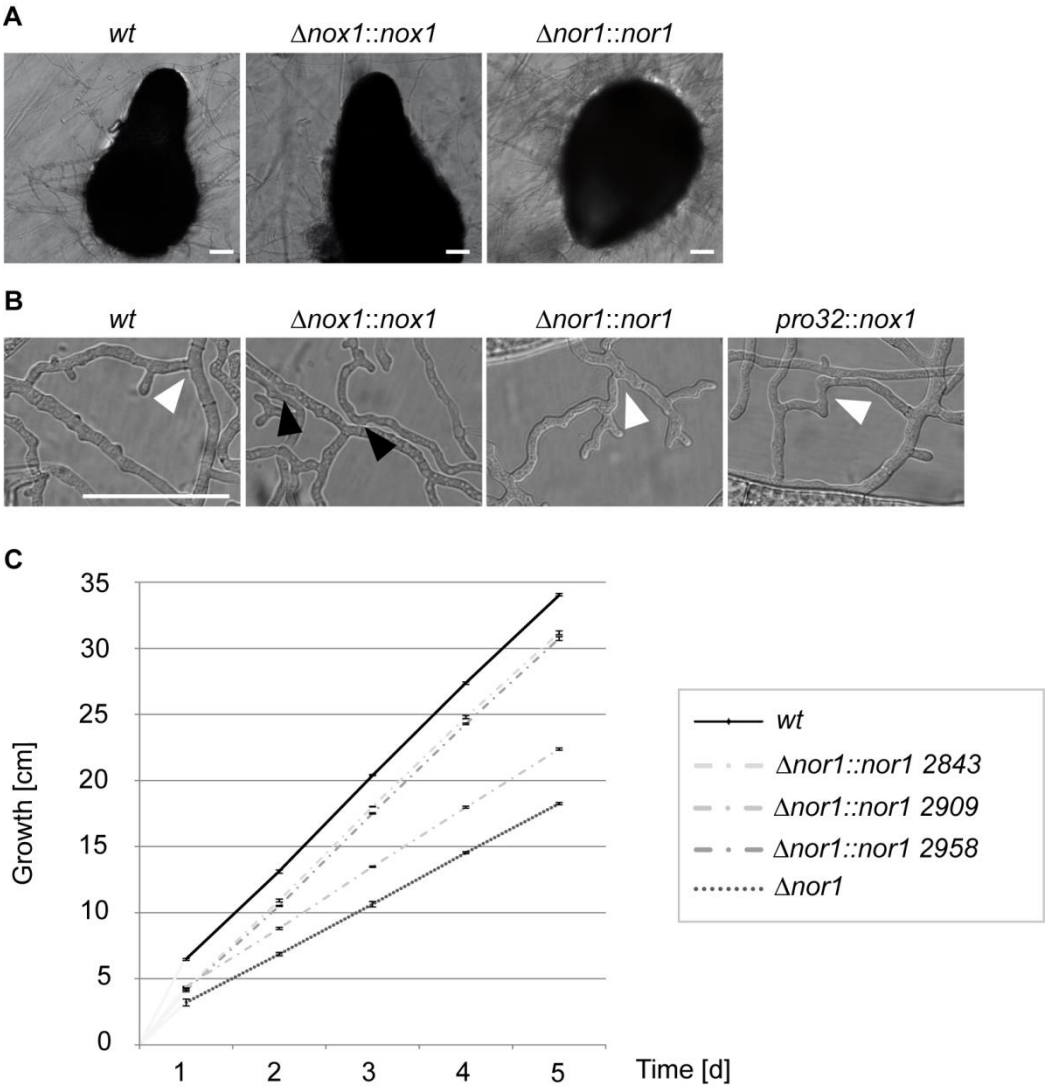

Figure S4 Phenotypes of complemented Δnox1, pro32 and Δnor1 mutants. (A) Complementation of Δnox1 and Δnor1 with the corresponding genes results in normal sexual development. The bar is 50 µm. (B) Hyphal fusion ability of pro32 and Δnor1 mutants was restored in Δnor1::*nor1* and pro32::*nox1* but not in fertile Δnox1::*nox1* complemented strains. Hyphal fusion is indicated by white arrowheads; the lack of hyphal fusion is marked by black arrowheads. The bar is 50 µm. (C) Normal growth was restored in Δnor1::*nor1* as it was in Δnox1::*nox1* complemented strains. Growth was followed in race tubes for 6 days in three replicates.

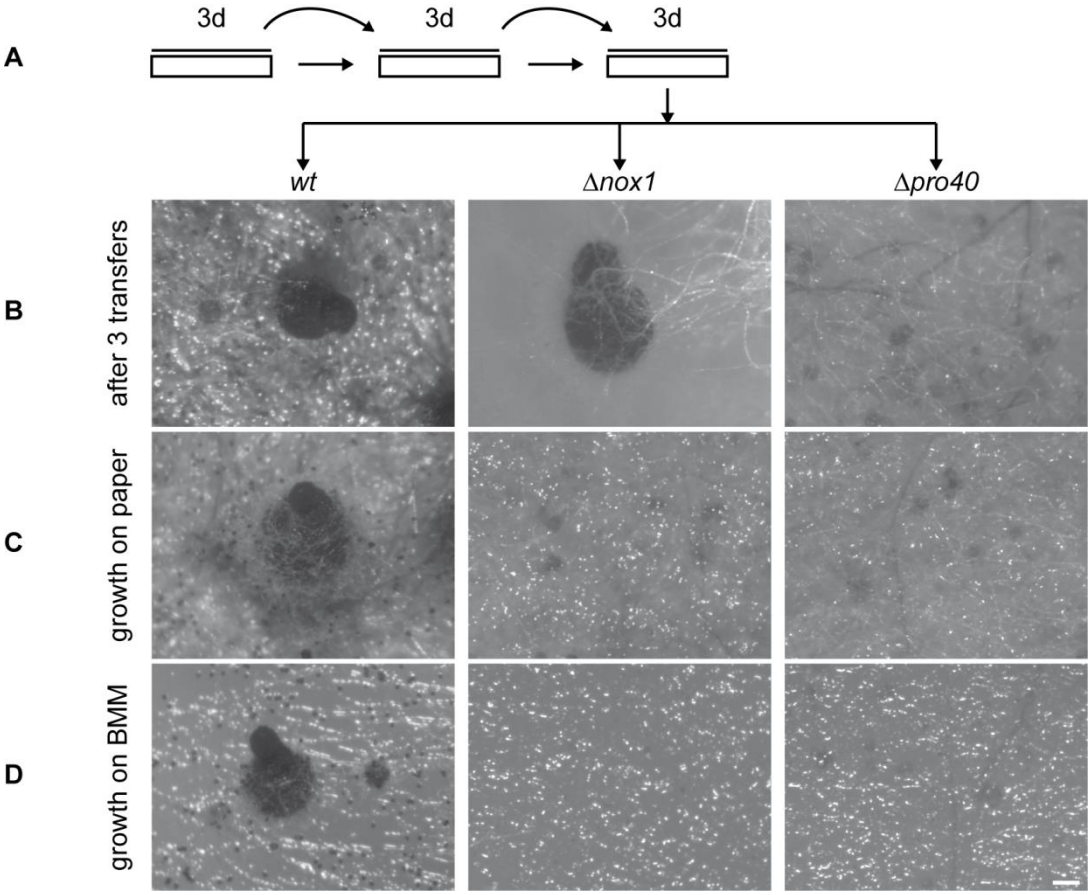

Figure S5 Restoration of Δnox1 fertility by a serial transfer to BMM medium. (A) Sceme to demonstrate the serial transfer of surface cultures on BMM medium. Strains were grown for 3 d on filter papers and subsequently transferred to fresh BMM media; (B) Growth of strains as indicated after 9 d. Serial transfers were done as depicted in (A); (C) Strains were grown for 9 d on filter papers layered on BMM medium; (D) Same as (C) without filter papers

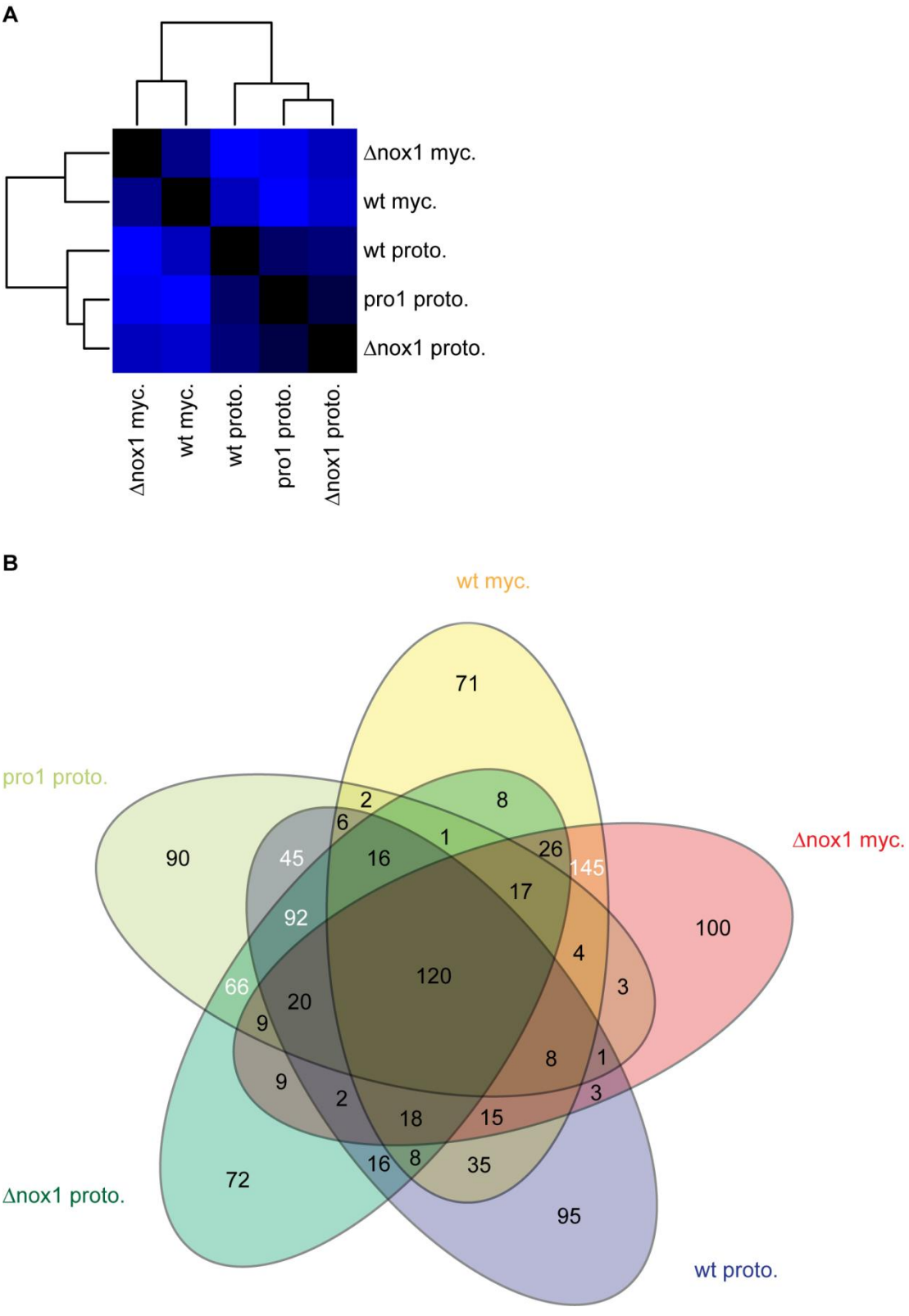

Figure S6 Expression patterns of protoperithecia are distinct from total mycelial samples. (A) Heatmap of correlation coefficients (Spearman) calculated from normalized read counts for classical analysis from protoperithecial (proto.) and mycelial (myc.) samples. Clustering and heatmap were done in R. (B) Venn diagrams of top 500 genes in different samples. Numbers of genes that are in the top 500 group for one or more or the five samples are given. In this analysis, only reads that map within 100 to 400 bases from the 3' end of the mRNA were used to account for the 3' bias in the microdissection samples and different mRNA lengths. Numbers for the four intersections containing the highest numbers of genes are indicated in white (not counting fields that represent genes occuring in all or only in one group). These intersections are wt mycelia and Δnox1 mycelia (145), wt protoperithecia and Δnox1 protoperithecia and pro1 protoperithecia (92), Δnox1 protoperithecia and pro1 protoperithecia (66), and wt protoperithecia and pro1 protoperithecia (45).

Files S1-S4

Available for download at http://www.genetics.org/lookup/suppl/doi:10.1534/genetics.113.159368/-/DC1

File S1 Analysis of raw read counts of *S. macrospora* genes obtained from RNA-seq analysis of mycelia and protoperithecia of Δnox1, pro1 and wild type.

File S2 Movie 1 Germination of fus spores. Ascospores were inoculated on BMM-Ac at 27°C. Ascospore germination was imaged with 5 min intervals for 60 min and analyzed with MetaMorph (version 7.7.5.0, Universal Imaging) software. Display rate, 1 frame /12 s. Related to Figure 5C.

File S3 Movie 2 Germination of Δnox2/fus spores. Ascospores were inoculated on BMM-Ac at 27°C. Ascospore germination was imaged with 5 min intervals for 60 min and analyzed with MetaMorph (version 7.7.5.0, Universal Imaging) software. Display rate, 1 frame /12 s. Related to Figure 5C.

File S4 Movie 3 Germination of Δgsa3Δnox2/fus spores. Ascospores were inoculated on BMM-Ac at 27°C. Ascospore germination was imaged with 5 min intervals for 60 min and analyzed with MetaMorph (version 7.7.5.0, Universal Imaging) software. Display rate, 1 frame /12 s. Related to Figure 5C.

Table S1 Summary of sequence reads generated from mutant and wild type samples

Sample	Total no. of reads	Read length in bases	Total MB	Coverage	No. of reads mapped to reference genome	% of reads mapped to reference genome
wt_3	108,513,967	51	5534	134x	105,047,645	96.8
pro32/fus	91,404,127	51	4662	114x	89,264,279	97.7

Table S2 Summary of sequence reads generated with RNA-seq analysis in this study

Condition	Sample	No. of reads	No. of reads mapped to reference genome	% of reads mapped to reference genome
wild type sexual mycelium	SM10	43,457,800	40,739,279	93.7
Δnox1 sexual mycelium	SM12	48,567,244	46,076,199	95.1
	SM15	58,330,616	55,736,653	95.6
Δnox1 protoperithecia	SM16	71,689,682	65,226,730	91.0
	SM17	65,178,132	60,057,518	92.1

Table S3 Cellular functions of differentially regulated genes in Δnox1 protoperithecia compared to wild type protoperithecia

Direction of regulation	*S. macrospora* locus tag	Gene designation	Cellular function of the corresponding protein in several organisms
Genes involved in cytoskeleton remodeling and hyphal fusion			
Upregulated	SMAC_00609	*ham-10*	Hyphal fusion[a]
	SMAC_00958	*profilin*	Profilin binds actin monomers[b]
	SMAC_02216	*cdc42*	Regulation of septin[c], STE20[d], NoxA localization[e], leads to actin assembly and polarized growth in response to pheromones[f]
	SMAC_02227	*crn-1*	Establishment of polarity, growth and stable Spitzenkörper[g]
	SMAC_02633	*rts-1*	Bud growth, accumulation of G1 cyclin[h]
	SMAC_04679	*rdi1*	Recycling of CDC42[i]
	SMAC_05207	*las17*	Stabilization of actin patches (endocytosis)[b]
	SMAC_07118	*dynactin 6*	Active transport along the microtubules[j]
	SMAC_04212	*kinesin*	Active transport along the microtubules[j]
	SMAC_06372	*kinesin*	Active transport along the microtubules[j]
	SMAC_07150	*kinesin*	Active transport along the microtubules[j]
	SMAC_07711	*kinesin*	Active transport along the microtubules[j]
Downregulated	SMAC_01612	*rax1*	Bipolar budding of dipoloid cells[k]
	SMAC_02720	*rsr1/bud1*	Localization[l] and regulation[m] CDC42
	SMAC_02963	*cbk1*	Septum disruption after cell division[n]
	SMAC_05949	*bem3*	GAP of CDC42[o]
	SMAC_09273	*cofilin*	De-polimerization of actin filaments[p]
Genes involved in ubiquitin mediated protein degradation or autophagy			
Upregulated	SMAC_01774	*ubiquitin-activating E1 1*	Ubiquitin binding[q]
	SMAC_03099	*ubiquitin-conjugating E*	Ubiquitin binding[q]
	SMAC_05013	*ubiquitin-conjugating E2 13*	Ubiquitin binding[q]
	SMAC_05407	*apc5*	Protein degradation[r]
	SMAC_05726	*pex4*	Ubiquitin binding[q]
	SMAC_06684	*cul-4*	Protein degradation[r]
	SMAC_06747	*ubiquitin-protein ligase gene*	Ubiquitin binding[q]
Downregulated	SMAC_06998	*atg12*	Autophagosome formation[s]
Genes involved in sexual development			
Upregulated	SMAC_00047	*fl*	Transcription factor[t]
	SMAC_02283	*pre-1*	Pheromone receptor[u]
	SMAC_05401	*SmtA-1*	Mating type factor[v]

	SMAC_05403	*SmtA-3*	Mating type factor[v]
Downregulated	SMAC_06479	*ste12*	Ascospore germination[w]
Genes involved in mitochondrial respiratory chain			
Upregulated	SMAC_01349	*nuo9.5*	Subunit of complex I (mitochondrial respiration)[x]
	SMAC_02450	*nuo78*	Subunit of complex I (mitochondrial respiration) [x]
	SMAC_04043	*nuo11.5*	Subunit of complex I (mitochondrial respiration[x]
	SMAC_04093	*cytochrome-c oxidase chain VIIc*	Cytochrome c oxidase of complex III (mitochondrial respiration)[y]
	SMAC_05824	*nuo49*	Subunit of complex I (mitochondrial respiration) [x]
	SMAC_07036	*nuo10.4*	Subunit of complex I (mitochondrial respiration) [x]
	SMAC_07180	*nuo21*	Subunit of complex I (mitochondrial respiration) [x]
	SMAC_08634	*nuo14*	Subunit of complex I (mitochondrial respiration) [x]
Downregulated	SMAC_12686	*ATP synthase subunit 6*	Mitochondrial ATPase[z]
	SMAC_12688	*ATP synthase subunit 9*	Mitochondrial ATPase[z]

[a](Fu *et al.* 2011); [b](Berepiki *et al.* 2011); [c](Dagdas *et al.* 2012); [d](Chen and Thorner 2007); [e](Semighini and Harris 2008); [f](Jones and Bennett 2011); [g](Echauri-Espinosa *et al.* 2012); [h](Artiles *et al.* 2009); [i](Das *et al.* 2013); [j](Rank and Rayment 2013); [k](Krappmann *et al.* 2007); [l](Pulver *et al.* 2013); [m](Park *et al.* 1997); [n](Brace *et al.* 2011); [o](Knaus *et al.* 2007); [p](Berepiki and Read 2013); [q](Strieter and Korasick 2012); [r](van der Veen and Ploegh 2012); [s](Iino and Noji 2013); [t](Bailey and Ebbole 1998); [u](Mayrhofer *et al.* 2006); [v](Klix *et al.* 2010); [w](Nolting and Pöggeler 2006); [x](Tanida 2011); [y](Duarte and Videira 2000); [z](Mavridou *et al.* 2013)

Table S4 Differentially regulated genes in Δnox1 protoperithecia compared to wild type protoperithecia with an impact on sexual development in *N. crassa*

S. macrospora locus tag	*N.crassa* locus tag	Gene designation	Gene product	Phenotype of *N. crassa* deletion mutant
upregulated in Δnox1 protoperithecia compared to wild type protoperithecia				
SMAC_00047	NCU_08726	*fl*	transcription factor fluffy	sterile[a]
SMAC_00190	NCU00911	*cps1*	Polysaccharide synthase Cps1p	sterile, reduced growth[a]
SMAC_00609	NCU02833	*ham-10*	Hyphal anastomosis-10	sterile, reduced growth, cell fusion deficient[b]
SMAC_02227	NCU00202	*crn*	Coronin-1	sterile, reduced growth, no polarity during germination[c]
SMAc_02283	NCU00138	*pre-1*	Pheromone receptor-1	female sterile[d]
SMAC_02450	NCU01765	*nuo78*	NADH:ubiquinone oxidoreductase 78	Reduced perithecia formation, no ascospore production[e]
SMAC_04395	NCU04198	*cac-1*	Chromatin assembly-1	Sterile, reduced growth[a]
SMAC_05401	NCU01958	*matA-1*	Mating type protein A-1	sterile, heterokaryon compatible[f]
SMAC_05403	NCU01960	*matA-3*	Mating type protein A-3	few ascospores formed[g]
SMAC_05824	NCU02534	*nuo49*	NADH:ubiquinone oxidoreductase 49	Sterile, reduced growth[e]
SMAC_06177	NCU04001	*ff-7*	Transcription factor female fertility-7	sterile[a]
SMAC_06684	NCU00272	*cul-4*	Cullin-4	sterile, reduced growth[a]
SMAC_07314	NCU07622		Putative GTPase activating protein	sterile[a]
SMAC_08994	NCU05758	*pre-2*	Pheromone receptor-2	sterile, no ascospore formation[a]
downregulated in Δnox1 protoperithecia compared to wild type protoperithecia				
SMAC_00010	NCU10142		Putative heterokaryon incompatibility protein	sterile[a]
SMAC_00177	NCU09211	*sad-3*	Suppressor of ascus dominance-3	no ascospore production[h]
SMAC_01666	NCU09915	*fsd-1*	Female sexual development-1	sterile, defect in ascospore

				maturation[a]
SMAC_02093	NCU07816		Putative magnesium and cobalt transporter CorA	sterile[a]
SMAC_02094	NCU07817	*ncw-3*	Non-anchored cell wall protein-3	sterile, reduced growth[a]
SMAC_06479	NCU00340	*pp-1*	protoperithecium-1	sterile, reduced growth, ascsospore germination defect[i]
SMAC_07309	NCU07617	*acon-3*	Aconidiate-3	sterile[a]
SMAC_07994	NCU08227		Putative glycosyl hydrolase	sterile[a]
SMAC_08793	NCU08739		endothiapepsin	sterile, reduced growth[a]
SMAC_12613	NCU07172	*stk-8*	Serine/threonine protein kinase-8	sterile, reduced growth, defective in conidia development[j]

[a]*Neurospora crassa* Sequencing Project, Broad Institute of Harvard and MIT (http://www.broadinstitute.org/); [b](Fu *et al.* 2011); [c](Echauri-Espinosa *et al.* 2012); [d](Kim and Borkovich 2004); [e](Tanida 2011); [f](Glass and Lee 1992); [g](Ferreira *et al.* 1998); [h](Hammond *et al.* 2012); [i](Li *et al.* 2005); [j](Park *et al.* 2011)

Artiles, K., S. Anastasia, D. McCusker, and D. R. Kellogg, 2009 The Rts1 regulatory subunit of protein phosphatase 2A is required for control of G1 cyclin transcription and nutrient modulation of cell size. PLoS Genet. 5: e1000727.

Bailey, L. A., and D. J. Ebbole, 1998 The *fluffy* gene of *Neurospora crassa* encodes a Gal4p-type C6 zinc cluster protein required for conidial development. Genetics 148: 1813-1820.

Berepiki, A., A. Lichius, and N. D. Read, 2011 Actin organization and dynamics in filamentous fungi. Nat. Rev. Microbiol. 9: 876-887.

Berepiki, A., and N. D. Read, 2013 Septins are important for cell polarity, septation and asexual spore formation in *Neurospora crassa* and show different patterns of localisation at germ tube tips. PLoS One 8: e63843.

Brace, J., J. Hsu, and E. L. Weiss, 2011 Mitotic exit control of the *Saccharomyces cerevisiae* Ndr/LATS kinase Cbk1 regulates daughter cell separation after cytokinesis. Mol. Cell. Biol. 31: 721-735.

Chen, R. E., and J. Thorner, 2007 Function and regulation in MAPK signaling pathways: lessons learned from the yeast *Saccharomyces cerevisiae*. Biochim. Biophys. Acta. 1773: 1311-1340.

Dagdas, Y. F., K. Yoshino, G. Dagdas, L. S. Ryder, E. Bielska *et al.*, 2012 Septin-mediated plant cell invasion by the rice blast fungus, *Magnaporthe oryzae*. Science 336: 1590-1595.

Das, A., B. D. Slaughter, J. R. Unruh, W. D. Bradford, R. Alexander *et al.*, 2013 Flippase-mediated phospholipid asymmetry promotes fast Cdc42 recycling in dynamic maintenance of cell polarity. Nat. Cell. Biol. 14: 304-310.

Duarte, M., and A. Videira, 2000 Respiratory chain complex I is essential for sexual development in Neurospora and binding of iron sulfur clusters are required for enzyme assembly. Genetics 156: 607-615.

Echauri-Espinosa, R. O., O. A. Callejas-Negrete, R. W. Roberson, S. Bartnicki-Garcia, and R. R. Mourino-Perez, 2012 Coronin is a component of the endocytic collar of hyphae of *Neurospora crassa* and is necessary for normal growth and morphogenesis. PLoS One 7: e38237.

Ferreira, A. V., Z. An, R. L. Metzenberg, and N. L. Glass, 1998 Characterization of *mat A-2*, *mat A-3* and Δ*matA* mating-type mutants of *Neurospora crassa*. Genetics 148: 1069-1079.

Fu, C., P. Iyer, A. Herkal, J. Abdullah, A. Stout *et al.*, 2011 Identification and characterization of genes required for cell-to-cell fusion in *Neurospora crassa*. Eukaryot. Cell 10: 1100-1109.

Glass, N. L., and L. Lee, 1992 Isolation of *Neurospora crassa A* mating type mutants by repeat induced point (RIP) mutation. Genetics 132: 125-133.

Hammond, T. M., D. G. Rehard, H. Xiao, and P. K. Shiu, 2012 Molecular dissection of Neurospora Spore killer meiotic drive elements. Proc. Natl. Acad. Sci. USA 109: 12093-12098.

Iino, R., and H. Noji, 2013 Operation mechanism of F(o) F(1)-adenosine triphosphate synthase revealed by its structure and dynamics. IUBMB Life 65: 238-246.

Jones, S. K., Jr., and R. J. Bennett, 2011 Fungal mating pheromones: choreographing the dating game. Fungal Genet. Biol. 48: 668-676.

Kim, H., and K. A. Borkovich, 2004 A pheromone receptor gene, *pre-1*, is essential for mating type-specific directional growth and fusion of trichogynes and female fertility in *Neurospora crassa*. Mol. Microbiol. 52: 1781-1798.

Klix, V., M. Nowrousian, C. Ringelberg, J. J. Loros, J. C. Dunlap *et al.*, 2010 Functional characterization of *MAT1-1*-specific mating-type genes in the homothallic ascomycete *Sordaria macrospora* provides new insights into essential and nonessential sexual regulators. Eukaryot. Cell 9: 894-905.

Knaus, M., M. P. Pelli-Gulli, F. van Drogen, S. Springer, M. Jaquenoud *et al.*, 2007 Phosphorylation of Bem2p and Bem3p may contribute to local activation of Cdc42p at bud emergence. Embo J. 26: 4501-4513.

Krappmann, A. B., N. Taheri, M. Heinrich, and H. U. Mösch, 2007 Distinct domains of yeast cortical tag proteins Bud8p and Bud9p confer polar localization and functionality. Mol. Biol. Cell 18: 3323-3339.

Li, D., P. Bobrowicz, H. H. Wilkinson, and D. J. Ebbole, 2005 A mitogen-activated protein kinase pathway essential for mating and contributing to vegetative growth in *Neurospora crassa*. Genetics 170: 1091-1104.

Mavridou, D. A., M. N. Clark, C. Choulat, S. J. Ferguson, and J. M. Stevens, 2013 Probing heme delivery processes in Cytochrome c biogenesis system I. Biochemistry 52: 7262-7270.

Mayrhofer, S., J. M. Weber, and S. Pöggeler, 2006 Pheromones and pheromone receptors are required for proper sexual development in the homothallic ascomycete *Sordaria macrospora*. Genetics 172: 1521-1533.

Nolting, N., and S. Pöggeler, 2006 A STE12 homologue of the homothallic ascomycete *Sordaria macrospora* interacts with the MADS box protein MCM1 and is required for ascosporogenesis. Mol. Microbiol. 62: 853-868.

Park, G., J. A. Servin, G. E. Turner, L. Altamirano, H. V. Colot *et al.*, 2011 Global analysis of serine-threonine protein kinase genes in *Neurospora crassa*. Eukaryot. Cell 10: 1553-1564.

Park, H. O., E. Bi, J. R. Pringle, and I. Herskowitz, 1997 Two active states of the Ras-related Bud1/Rsr1 protein bind to different effectors to determine yeast cell polarity. Proc. Natl. Acad. Sci. USA 94: 4463-4468.

Pulver, R., T. Heisel, S. Gonia, R. Robins, J. Norton *et al.*, 2013 Rsr1 focuses Cdc42 activity at hyphal tips and promotes maintenance of hyphal development in *Candida albicans*. Eukaryot. Cell 12: 482-495.

Rank, K. C., and I. Rayment, 2013 Functional asymmetry in kinesin and dynein dimers. Biol. Cell 105: 1-13.

Semighini, C. P., and S. D. Harris, 2008 Regulation of apical dominance in *Aspergillus nidulans* hyphae by reactive oxygen species. Genetics 179: 1919-1932.

Strieter, E. R., and D. A. Korasick, 2012 Unraveling the complexity of ubiquitin signaling. ACS Chem. Biol. 7: 52-63.

Tanida, I., 2011 Autophagosome formation and molecular mechanism of autophagy. Antioxid. Redox Signal. 14: 2201-2214.

van der Veen, A. G., and H. L. Ploegh, 2012 Ubiquitin-like proteins. Annu. Rev. Biochem. 81: 323-357.